

# Clustering coefficients for networks with higher order interactions

Gyeong-Gyun Ha (하경균) <sup>1</sup>, Izaak Neri <sup>1</sup> and Alessia Annibale <sup>1</sup>  
*Department of Mathematics, King's College London, Strand, London, WC2R 2LS, UK*

(\*Electronic mail: gyeong-gyun.ha@kcl.ac.uk)

(Dated: 20 February 2024)

We introduce a clustering coefficient for nondirected and directed hypergraphs, which we call the *quad clustering coefficient*. We determine the average quad clustering coefficient and its distribution in real-world hypergraphs and compare its value with those of random hypergraphs drawn from the configuration model. We find that real-world hypergraphs exhibit a nonnegligible fraction of nodes with a maximal value of the quad clustering coefficient, while we do not find such nodes in random hypergraphs. Interestingly, these highly clustered nodes can have large degrees and can be incident to hyperedges of large cardinality. Moreover, highly clustered nodes are not observed in an analysis based on the pairwise clustering coefficient of the associated projected graph that has binary interactions, and hence higher order interactions are required to identify nodes with a large quad clustering coefficient.

**Real-world networks exhibit, so-called, higher order interactions, which are relations that involve more than two parties. Such higher order interactions can be represented by hyperedges, and a collection of nodes and hyperedges is called a hypergraph. The question arises what are the topological properties of real-world systems that have higher order interactions, such as, social collaboration networks or product composition networks. This problem is challenging as real-world networks can consist of a large number of nodes and hyperedges. Moreover, hyperedges in real-world networks can connect up to hundreds of nodes. To address the topological properties of hypergraphs, we introduce in this Paper a clustering coefficient that determines the density of quads incident to a node, and which we call the quad clustering coefficient. Comparing the quad clustering coefficients of nodes in real-world networks with those in random networks, we find that real-world systems have topological properties that are significantly different from those of random systems. Notably, real-world hypergraphs have a large fraction of nodes with a maximal value of the quad clustering coefficient. This feature is only observed when accounting for the higher order interactions and is not seen in a classical network analysis based on binary interactions. We believe that these results are interesting for developing more accurate null models for real-world networks with higher order interactions.**

tion of cardinality  $\chi$ .

Although in a first approximation real-world networks appear to be random, random networks have a smaller number of cliques than what is observed in real-world networks<sup>1-3</sup>. Indeed, the average clustering coefficient of a random graph, measuring the density of triangles<sup>5</sup> (the smallest possible clique), decreases linearly as a function of the number of nodes in the graph. On the other hand, the average clustering coefficient of real-world networks is larger and approximately independent of  $N$ <sup>6</sup>. Because of this observation, more realistic models for real-world networks have been developed that are based on a hierarchical network<sup>7</sup> or a small-world network structure<sup>5,8</sup>.

For systems with higher order interactions, Refs.<sup>9-12</sup> define a clustering coefficient that measures the degree of local transitivity, and corresponds with quantifying clustering of nodes in the projected graph associated with a higher order network. However, contrarily to the case of simple graphs, the clustering coefficients of Refs.<sup>9-13</sup> do not capture the density of the shortest cycles in hypergraphs.

In this Paper, we propose an alternative observable for clustering in hypergraphs that quantifies the density of the shortest possible simple cycle. The shortest simple cycle of a hypergraph is a quad. In a bipartite representation of a hypergraph, where nodes and hyperedges represent the two parties of the bipartite graph, a quad is a closed path of length four consisting of an alternating sequence of two nodes and two hyperedges. The quad clustering coefficient that we introduce in this paper quantifies the density of quads and it is reminiscent of clustering coefficients that quantify densities of squares in bipartite graphs, see Refs.<sup>14-16</sup>, but there are also some notable distinctions. For example, as we show here, the quad clustering coefficient is more effective in quantifying the density of quads in a hypergraph than coefficients defined previously in the literature. After a comparison with these previous works, we study clustering of quads in random graphs and real-world networks.

The paper is structured as follows. In Sec. II, we define hypergraphs and introduce the notation used in this paper. In Sec. III, we define the quad clustering coefficient and compare this coefficient with similar coefficients studied in the context of bipartite graphs. In Sec. IV, we derive exact expressions of

## I. INTRODUCTION

Networks consist of nodes, representing components of a system, and relations between those nodes. When the relations are binary, they can be represented as links in a graph<sup>1-3</sup>. However in real-world systems relations often include three or more vertices, and these are called higher order interactions<sup>4</sup>. For example, a protein-protein interaction network can be seen as a network of binary relations, where two proteins are connected when they bind to each other, or it can be seen as a network with higher order interactions where a protein complex of  $\chi$  proteins corresponds to a higher order interac-

the ensemble average of the quad clustering coefficient in a random hypergraph model. In Sec. V, we compare the results of Sec. IV with real-world hypergraphs and discuss notable distinctions between real-world networks and random graphs. In Sec. VI, we extend the quad clustering coefficient to directed hypergraphs, and make a corresponding study for real-world networks. Conclusions are given in Sec. VII, and the Paper ends with several Appendices containing technical details on the calculations in this Paper.

## II. PRELIMINARIES ON HYPERGRAPHS

A nondirected, hypergraph is a triplet  $\mathcal{H} = (\mathcal{V}, \mathcal{W}, \mathcal{E})$  consisting of a set  $\mathcal{V}$  of  $N = |\mathcal{V}|$  nodes, a set of  $\mathcal{W}$  of  $M = |\mathcal{W}|$  hyperedges, and a set  $\mathcal{E}$  of links. We denote nodes by roman indices,  $i, j \in \mathcal{V}$ , and hyperedges by Greek indices  $\alpha, \beta \in \mathcal{W}$ . The set of links  $\mathcal{E}$  consists of pairs  $(i, \alpha)$  with  $i \in \mathcal{V}$  and  $\alpha \in \mathcal{W}$ . We say that the hypergraph is *simple* when each pair  $(i, \alpha)$  occurs at most once in the set  $\mathcal{E}$ .

A simple, nondirected hypergraph can be represented by an *incidence matrix* of dimensions  $N \times M$  that is defined by

$$[\mathbf{I}]_{i\alpha} \equiv \begin{cases} 1 & \text{if } (i, \alpha) \in \mathcal{E}, \\ 0 & \text{if } (i, \alpha) \notin \mathcal{E}. \end{cases} \quad (1)$$

Consequently, a hypergraph can also be represented as a bipartite graph whose vertices are the nodes and the hyperedges of the hypergraph. Figure 1 shows an example of a hypergraph represented as a bipartite graph and an incidence matrix. For simplicity, we often make no distinction between the hypergraph  $\mathcal{H}$  and its representation  $\mathbf{I}$ .

We define the network observables that we use in this Paper. The *degree* of node  $i \in \mathcal{V}$  is defined by

$$k_i(\mathbf{I}) \equiv \sum_{\alpha=1}^M I_{i\alpha}, \quad (2)$$

and we use the vector notation

$$\vec{k}(\mathbf{I}) \equiv (k_1(\mathbf{I}), k_2(\mathbf{I}), \dots, k_N(\mathbf{I})) \quad (3)$$

to denote the sequence of degrees of the hypergraph  $\mathbf{I}$ . Analogously, we define the *cardinality* of a hyperedge  $\alpha$  by

$$\chi_\alpha(\mathbf{I}) \equiv \sum_{i=1}^N I_{i\alpha}, \quad (4)$$

and the sequence of cardinalities is

$$\vec{\chi}(\mathbf{I}) \equiv (\chi_1(\mathbf{I}), \chi_2(\mathbf{I}), \dots, \chi_M(\mathbf{I})). \quad (5)$$

As a hypergraph is a graph with higher order interactions, we also consider the degrees

$$k_i(\mathbf{I}; \chi) = \sum_{\alpha=1}^M I_{i\alpha} \delta_{\chi_\alpha(\mathbf{I}), \chi} \quad (6)$$

that determine the number of hyperedges of cardinality  $\chi$  that are incident to node  $i$ . In (6)  $\delta_{n,m}$ , with  $n, m \in \mathbb{N}$ , represents

the Kronecker-delta function. We denote the number of hyperedges incident to node  $i$ , excluding those with cardinality 1, by the so-called *modified degree*

$$k_i^*(\mathbf{I}) \equiv \sum_{\chi=2}^{\infty} k_i(\mathbf{I}; \chi). \quad (7)$$

Lastly, we define the neighbourhood set

$$\partial_{i\alpha}(\mathbf{I}) \equiv \{j \in \mathcal{V} \mid I_{i\alpha} I_{j\alpha} \neq 0\} \quad (8)$$

consisting of nodes that are incident to the hyperedge  $\alpha$  that is connected to the node  $i$ .

When  $\chi_\alpha(\mathbf{I}) = 2$  for all  $\alpha \in \mathcal{W}$ , then  $\mathbf{I}$  represents a graph. In this case, we can also represent the graph in terms of the adjacency matrix  $\mathbf{A}$  with off-diagonal entries

$$A_{ij} = \sum_{\alpha=1}^M I_{i\alpha} I_{j\alpha} \quad (9)$$

and zero-valued diagonal entries,  $A_{ii} = 0$ . We say that the graph is simple when  $A_{ij} \in \{0, 1\}$ .

Given a hypergraph, we can define the so-called *projected graph* by the adjacency matrix  $\mathbf{A}^{\text{proj}}$  with entries

$$A_{ij}^{\text{proj}} = \Theta \left( \sum_{\alpha=1}^M I_{i\alpha} I_{j\alpha} \right) \quad (10)$$

where  $\Theta(x)$  is the Heaviside function, i.e.,  $\Theta(x) = 1$  when  $x > 0$  and  $\Theta(x) = 0$  when  $x \leq 0$ . Note that this map is surjective, as a projected graph can correspond with multiple hypergraphs.

## III. QUAD CLUSTERING COEFFICIENT: DEFINITION AND MOTIVATION

For simple graphs with pairwise interactions determined by the adjacency matrix  $\mathbf{A}$ , the clustering coefficient of a node with degree  $k_i(\mathbf{A}) \geq 2$  is given by<sup>5</sup>

$$C_i^{\text{pi}}(\mathbf{A}) \equiv \frac{T_i(\mathbf{A})}{t_{\max}(k_i(\mathbf{A}))}, \quad (11)$$

where  $T_i(\mathbf{A})$  is the number of triangles incident to node  $i$ , and

$$t_{\max}(k_i(\mathbf{A})) = \frac{k_i(\mathbf{A})(k_i(\mathbf{A}) - 1)}{2} \quad (12)$$

is the maximum possible number of triangles incident to a node with degree  $k_i(\mathbf{A})$ . Hence, the clustering coefficient  $C_i^{\text{pi}}$  determines the density of triangles incident to node  $i$ . If  $C_i^{\text{pi}} = 1$ , then all possible triangles incident to node  $i$  are present, and if  $C_i^{\text{pi}} = 0$  then none of the triangles are present. If  $k_i \leq 1$ , then by convention we set  $C_i^{\text{pi}} = 0$ .

Since a triangle is the shortest cycle in a simple graph, the clustering coefficient  $C_i^{\text{pi}}$  is the density of shortest cycles incident to a node  $i$ , and we use this property of the clustering coefficient for graphs with pairwise interactions to derive a

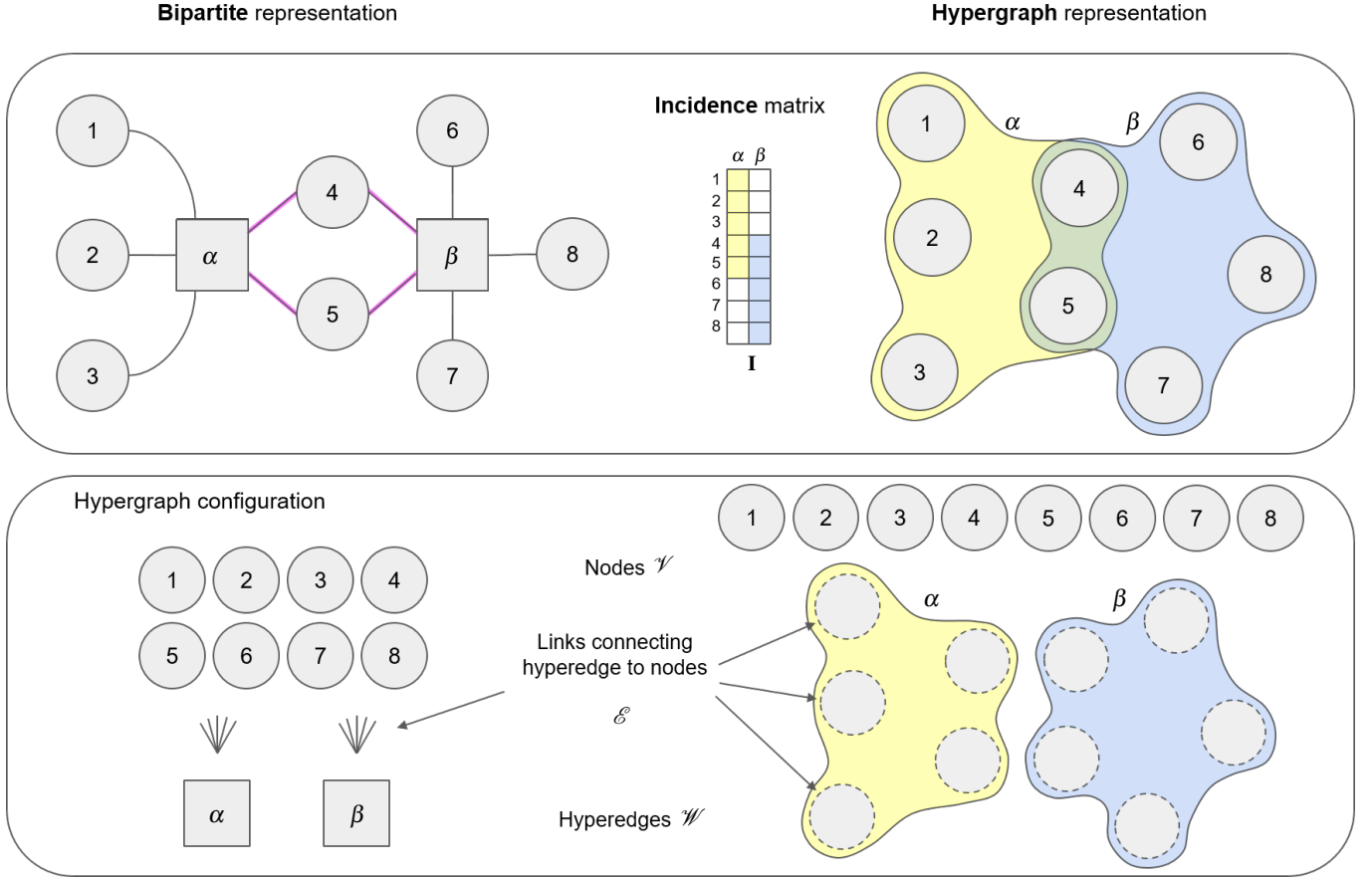


FIG. 1: *Illustration of a hypergraph, its different representations, and the quad motif.* The upper panel shows the three ways of representing a hypergraph, namely, as a bipartite graph, as an incidence matrix, and as a graph with higher order interactions. The illustrated hypergraph in the left top panel has one quad, highlighted in magenta, consisting of the hyperedges  $\alpha$  and  $\beta$  and the nodes 4 and 5. The lower panel visualises the three different components of a hypergraph, namely, the set of nodes  $\mathcal{V}$ , the set of links  $\mathcal{E}$ , and the set of hyperedges  $\mathcal{W}$ .

clustering coefficient valid for hypergraphs. To this aim, we represent a hypergraph as a bipartite graph, see Fig. 1. In this bipartite representation, there exist no triangles, and instead the cycle of shortest length is a *quad* consisting of two nodes and two hyperedges, see the motif illustrated in magenta in Fig. 1 for an illustration of the quad. Specifically, the quad is a simple cycle of four links forming an alternating sequence of nodes and hyperedges.

#### A. Definition of the quad clustering coefficient

In this Section, we define the quad clustering coefficient  $C_i^q(\mathbf{I})$  of a node  $i$  in a hypergraph. Let  $i$  be a node that is connected to two or more hyperedges of cardinality two or higher, i.e.,  $k_i^*(\mathbf{I}) \geq 2$ . We define the quad clustering coefficient of  $i$  by

$$C_i^q(\mathbf{I}) \equiv \frac{Q_i(\mathbf{I})}{q_{\max}(\{k_i(\mathbf{I}; \chi)\}_{\chi \in \mathbb{N}})}, \quad (13)$$

where

$$Q_i(\mathbf{I}) \equiv \sum_{\alpha < \beta} q_{i\alpha\beta}(\mathbf{I}) \quad (14)$$

is the number of quads incident to node  $i$ , with  $\sum_{\alpha < \beta} = \sum_{\alpha=1}^M \sum_{\beta=\alpha+1}^M$  and

$$q_{i\alpha\beta}(\mathbf{I}) \equiv \sum_{j=1; j \neq i}^N I_{j\alpha} I_{j\beta} I_{i\alpha} I_{i\beta}, \quad (15)$$

and where

$$q_{\max}(\{k_i(\mathbf{I}; \chi)\}_{\chi \in \mathbb{N}}) \equiv \sum_{\alpha < \beta} \min\{\chi_\alpha(\mathbf{I}) - 1, \chi_\beta(\mathbf{I}) - 1\} I_{i\alpha} I_{i\beta} \quad (16)$$

is the maximal possible number of quads that a node with degrees  $\{k_i(\mathbf{I}; \chi)\}_{\chi \in \mathbb{N}}$  can have. In Appendix A we show that the maximal number of quads can also be expressed by

$$q_{\max} = \frac{1}{2} \sum_{\chi=2}^{\infty} (\chi - 1) k_i(\mathbf{I}; \chi) \left( \sum_{\chi'=2}^{\infty} k_i(\mathbf{I}; \chi') - 1 \right), \quad (17)$$

which makes it evident that  $q_{\max}$  is fully determined by the set  $\{k_i(\mathbf{I}; \chi)\}_{\chi \in \mathbb{N}}$  of degrees associated with node  $i$ . If  $k_i^*(\mathbf{I}) < 2$ , then  $C_i^q(\mathbf{I}) = 0$ , as the number of quads incident to a node with a degree less than two equals zero. Note that the formula for the maximal possible number of quads,  $q_{\max}$ , assumes that both the degree of node  $i$  and the cardinalities of the hyperedges connected to  $i$  are given. Also, note that the quad clustering coefficient is a density, i.e.,  $C_i^q(\mathbf{I}) \in [0, 1]$ , and in the example of Fig. 2,  $C_i^q(\mathbf{I}) = 0$ ,  $C_i^q(\mathbf{I}) = 1/2$  and  $C_i^q(\mathbf{I}) = 1$ .

The quad clustering coefficient  $C_i^q$  has two useful properties. First, for fixed degrees  $k_i(\mathbf{I}; \chi)$ , the quad clustering coefficient is a *linear function* of  $Q_i$ . Second, the proportionality factor is such that  $C_i^q \in [0, 1]$ , and  $C_i^q = 1$  is attained when the number of quads around the node  $i$  is maximal. As will become evident, these properties do not hold for clustering coefficients of bipartite graphs considered previously in the literature.

Note that quads quantify the multitude of ways neighbouring nodes interact with each other, and in simple graphs we need higher order interactions to have multiple interaction paths. In the case of simple graphs (i.e., all hyperedges have cardinality 2 and for each pair of nodes there is at most one hyperedge connecting them) the quad clustering coefficient is zero, as the only way to create multiple interactions between two nodes is through multiple edges, which are absent when the graph is simple.

In the next two Subsections, we compare the quad clustering coefficient with two other clustering coefficients for bipartite graphs, namely, Lind's clustering coefficient<sup>14</sup> in Sec. III B and Zhang's clustering coefficient<sup>15</sup> in Sec. III C. As we will see, Lind's and Zhang's clustering coefficients are not functions of  $Q_i$ , except when  $k_i = 2$ , and in the latter case Lind's and Zhang's clustering coefficients are nonlinear functions in  $Q_i$ . In addition to Lind's and Zhang's clustering coefficients, other clustering coefficients have been defined in the literature, see Refs.<sup>17–21</sup>, but since these are significantly different from the quad clustering coefficient we do not discuss them here. Specifically, the clustering coefficients in Refs.<sup>17,18</sup> apply to nodes in standard networks without higher order interactions, the clustering coefficient in Ref.<sup>19</sup> has a denominator that does not depend on the cardinalities of the hyperedges incident to the considered node, and the coefficients in Ref.<sup>20,21</sup> do not count the number of quads.

## B. Lind's clustering coefficient

In Ref.<sup>14</sup>, Lind, González, and Herrmann define a clustering coefficient by

$$C_i^{\text{Lind}}(\mathbf{I}) \equiv \frac{Q_i(\mathbf{I})}{q_{i,\max}^{\text{Lind}}(\mathbf{I})}, \quad (18)$$

where

$$q_{i,\max}^{\text{Lind}}(\mathbf{I}) \equiv \sum_{\alpha < \beta} [(\chi_\alpha(\mathbf{I}) - \eta_{i\alpha\beta}(\mathbf{I}))(\chi_\beta(\mathbf{I}) - \eta_{i\alpha\beta}(\mathbf{I})) + q_{i\alpha\beta}(\mathbf{I})] I_{i\alpha} I_{i\beta} \quad (19)$$

with

$$\eta_{i\alpha\beta}(\mathbf{I}) \equiv 1 + q_{i\alpha\beta}(\mathbf{I}). \quad (20)$$

For simplicity we call  $C_i^{\text{Lind}}(\mathbf{I})$  Lind's clustering coefficient. In the example of Fig. 2,  $C_i^{\text{Lind}}(\mathbf{I}) = 0$  for (a),  $C_i^{\text{Lind}}(\mathbf{I}) = 1/3$  for (b) and  $C_i^{\text{Lind}}(\mathbf{I}) = 1$  for (c).

The difference between the formulas for  $C_i^{\text{Lind}}(\mathbf{I})$  and  $C_i^q(\mathbf{I})$ , given by Eqs. (13) and (18), respectively, is in the definition of the maximal possible number of quads. For Lind's clustering coefficient,  $q_{i,\max}^{\text{Lind}}$  is the sum of the existing quads  $q_i$  and the number of ways  $(\chi_\alpha(\mathbf{I}) - \eta_{i\alpha\beta}(\mathbf{I}))(\chi_\beta(\mathbf{I}) - \eta_{i\alpha\beta}(\mathbf{I}))$  that the remaining edges can be combined to form quads. In general, the number  $q_{i,\max}^{\text{Lind}}$  overcounts significantly the number of possible quads. For example, in Fig. 2  $q_{i,\max}^{\text{Lind}} = 3$ , even though  $q_{\max} = 2$ .

Another notable difference between the quad clustering coefficient and Lind's clustering coefficient is that the former is a linear function of  $Q_i$ , while the latter is, in general, not a function of  $Q_i$ . An exception is when  $k_i = 2$ , in which case Lind's clustering coefficient is a function of  $Q_i$ , but this function is nonlinear. This feature is illustrated in the upper panel of Fig. 3 that plots Lind's clustering coefficient as a function of the quad clustering coefficient for a node of degree 2 that is connected to a hyperedge with cardinality  $\chi_\alpha$  and a hyperedge with cardinality  $\chi_\beta$ . The solid lines in Fig. 3 are obtained by taking the limit  $\chi_\alpha \rightarrow \infty$  with the ratio  $r = \chi_\beta/\chi_\alpha > 1$  fixed, yielding the function

$$C_i^{\text{Lind}}(q) = \lim_{\chi_\alpha \rightarrow \infty} C_i^{\text{Lind}}(\mathbf{I}) = \frac{q}{\chi_\alpha(1-q)(r-q) + q}, \quad (21)$$

where  $q = Q_i/(\chi_\alpha - 1) \in [0, 1]$  (see Appendix B). We observe a strong nonlinearity in  $C_i^{\text{Lind}}(q)$  for large values of  $\chi_\alpha$ . Indeed, as shown in Fig. 3(a), for  $q$  below one and large enough values of  $\chi_\alpha$ , it holds that  $C_i^{\text{Lind}}(q) \approx 0$ , and for  $q = 1$  it holds that  $C_i^{\text{Lind}}(q) = 1$ , which can be recovered from Eq. (21) by taking the limit  $\chi_\alpha \rightarrow \infty$ .

For nodes with a degree  $k_i > 2$ , Lind's clustering coefficient, is not a function of  $Q_i$ , contrarily to the quad clustering coefficient, as  $q_{i,\max}^{\text{Lind}}$  depends on all  $q_{i\alpha\beta}$ , with  $\alpha, \beta \in \mathcal{H}$ . For the simplest case of  $k_i = 3$ , we illustrate this feature in the lower panel of Fig. 3. The circles and squares denote  $C_i^{\text{Lind}}$  for two different assignments for  $q_{i\alpha\beta}$ ,  $q_{i\alpha\gamma}$ , and  $q_{i\beta\gamma}$ , as detailed in Appendix C. As Fig. 3(b) shows, the two curves for  $C_i^{\text{Lind}}$  are different for different prescriptions on the  $q$ 's indicating that  $C_i^{\text{Lind}}$  is not a function of  $Q_i$ .

## C. Zhang's clustering coefficient

In Ref.<sup>15</sup>, Zhang et al. introduce the clustering coefficient

$$C_i^{\text{Zhang}}(\mathbf{I}) \equiv \frac{Q_i(\mathbf{I})}{q_{i,\max}^{\text{Zhang}}(\mathbf{I})}, \quad (22)$$

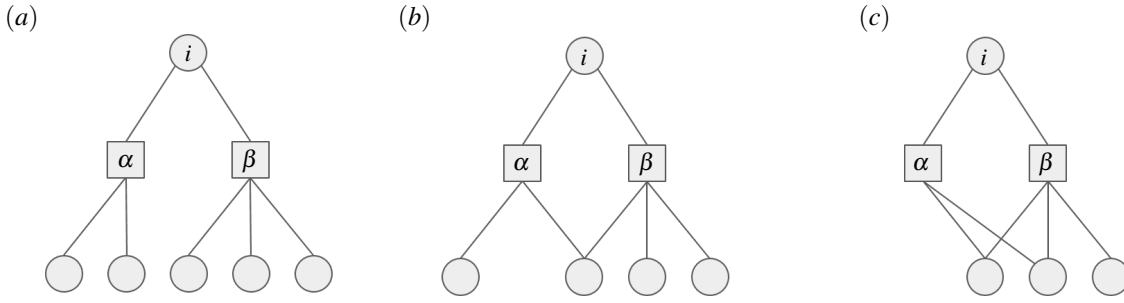


FIG. 2: The quad clustering coefficient of a node in a few simple examples. Node  $i$  is connected to hyperedges  $\alpha$  and  $\beta$  with cardinalities 3 and 4, respectively. Depending on the number of quads,  $C_i^q$  equals 0 (a),  $1/2$  (b), and 1 (c), respectively.

where

$$q_{i,\max}^{\text{Zhang}}(\mathbf{I}) = \sum_{\alpha < \beta} [(\chi_\alpha(\mathbf{I}) - \eta_{i\alpha\beta}(\mathbf{I})) + (\chi_\beta(\mathbf{I}) - \eta_{i\alpha\beta}(\mathbf{I})) + q_{i\alpha\beta}(\mathbf{I})] I_{i\alpha} I_{i\beta} \quad (23)$$

is the maximal possible number of quads. We call  $C_i^{\text{Zhang}}$  Zhang's clustering coefficient. Note that Zhang's clustering coefficient can also be written as<sup>16</sup>

$$C_i^{\text{Zhang}}(\mathbf{I}) = \frac{\sum_{\alpha, \beta; \alpha < \beta} |\partial_{i\alpha}(\mathbf{I}) \cap \partial_{i\beta}(\mathbf{I})|}{\sum_{\alpha, \beta; \alpha < \beta} |\partial_{i\alpha}(\mathbf{I}) \cup \partial_{i\beta}(\mathbf{I})|}, \quad (24)$$

which is known as the Jaccard similarity coefficient<sup>22</sup>.

Comparing  $C_i^{\text{Zhang}}(\mathbf{I})$  with  $C_i^{\text{Lind}}(\mathbf{I})$  and  $C_i^q(\mathbf{I})$ , we see that Zhang et al. considered yet another way of counting the maximal, possible number of quads. In the example of Fig. 2, we get  $C_i^{\text{Zhang}}(\mathbf{I}) = 0$  for (a),  $C_i^{\text{Zhang}}(\mathbf{I}) = 1/4$  for (b) and  $C_i^{\text{Zhang}}(\mathbf{I}) = 2/3$  for (c).

Like Lind's clustering coefficient, for nodes with degree  $k_i = 2$  Zhang's clustering coefficient is a nonlinear function of  $Q_i$ . Indeed, taking the limit  $\chi_\alpha \rightarrow \infty$  while keeping  $r = \chi_\alpha / \chi_\beta > 1$  fixed, we get

$$C_i^{\text{Zhang}}(q) = \lim_{\chi_\alpha \rightarrow \infty} C_i^{\text{Zhang}}(\mathbf{I}) = \frac{q}{1+r-q}, \quad (25)$$

for  $q \in [0, 1]$  (see Appendix B). We illustrate this function in the upper panel of Fig. 3. Note that Zhang's clustering coefficient is not normalised, as  $C_i^{\text{Zhang}}(1) = 1/r$ , and more generally  $C_i^{\text{Zhang}}(\mathbf{I}) \in [0, 1/\Gamma_i(\mathbf{I})]$ , with

$$\Gamma_i(\mathbf{I}) = \frac{\sum_{\alpha < \beta} \max\{\chi_\alpha(\mathbf{I}) - 1, \chi_\beta(\mathbf{I}) - 1\} I_{i\alpha} I_{i\beta}}{\sum_{\alpha < \beta} \min\{\chi_\alpha(\mathbf{I}) - 1, \chi_\beta(\mathbf{I}) - 1\} I_{i\alpha} I_{i\beta}}. \quad (26)$$

For nodes with degrees  $k_i > 2$ ,  $C_i^{\text{Zhang}}$  is not a function of  $Q_i$ , as  $q_{i,\max}^{\text{Zhang}}$  depends on  $q_{i\alpha\beta}$  for all  $\alpha, \beta \in \mathscr{H}$ .

#### IV. AVERAGE QUAD CLUSTERING COEFFICIENT FOR RANDOM HYPERGRAPHS

In this Section, we determine the average quad clustering coefficients for random hypergraphs. First, in Sec. IV A we

derive the ensemble averaged clustering coefficient in random hypergraph models with regular cardinalities, i.e.,  $\chi_\alpha(\mathbf{I}) = \chi$  for all  $\alpha \in \mathscr{H}$ . For these models we obtain compact expressions for the ensemble averaged quad clustering coefficient in terms of the model parameters. Subsequently, in Sec. IV B we deal with models that are biregular in the cardinalities, i.e.,  $\chi_\alpha(\mathbf{I}) \in \{\chi_1, \chi_2\}$ , and, as will become evident, the calculations in biregular models are significantly more difficult than those in models with regular cardinalities.

##### A. Regular cardinalities

We consider three random hypergraph models with regular cardinalities, i.e., for which  $\chi_\alpha(\mathbf{I}) = \chi$  for all  $\alpha \in \mathscr{H}$ . The three models are distinguished by the fluctuations in their degrees  $k_i(\mathbf{I})$ . In the  $\chi$ -regular ensemble, considered in Sec. IV A 1, the degrees are unconstrained; in the  $(k, \chi)$ -regular ensemble, considered in Sec. IV A 2, the degrees are regular, i.e.,  $k_i(\mathbf{I}) = k$  for all  $i \in \mathscr{V}$ ; lastly, in the  $(\vec{k}, \chi)$ -regular ensemble, considered in Sec. IV A 3, the degrees are prescribed by the sequence  $\vec{k}$ , i.e.,  $k_i(\mathbf{I}) = k_i$  for all  $i \in \mathscr{V}$ .

##### 1. $\chi$ -regular ensemble

In the  $\chi$ -regular ensemble the probability of drawing a hypergraph with incidence matrix  $\mathbf{I} \in \{0, 1\}^{NM}$  is given by

$$P_\chi(\mathbf{I}) \equiv \frac{1}{\mathcal{N}_\chi} \prod_{\alpha=1}^M \delta_{\chi, \chi_\alpha(\mathbf{I})}, \quad (27)$$

with the normalisation constant  $\mathcal{N}_\chi$  as derived in Appendix D 1.

The average quad clustering coefficient

$$\langle C_i^q(\mathbf{I}) \rangle_\chi \equiv \sum_{\mathbf{I}} P_\chi(\mathbf{I}) C_i^q(\mathbf{I}), \quad (28)$$

where  $\sum_{\mathbf{I}}$  is a sum over all possible incidence matrices  $\mathbf{I} \in \{0, 1\}^{NM}$ , is given by (see Appendix D 1 for a derivation)

$$\langle C_i^q(\mathbf{I}) \rangle_\chi = \frac{\chi - 1}{N - 1} \left[ 1 - \left( 1 - \frac{\chi}{N} \right)^M \left( 1 + \frac{M\chi}{N - \chi} \right) \right]. \quad (29)$$

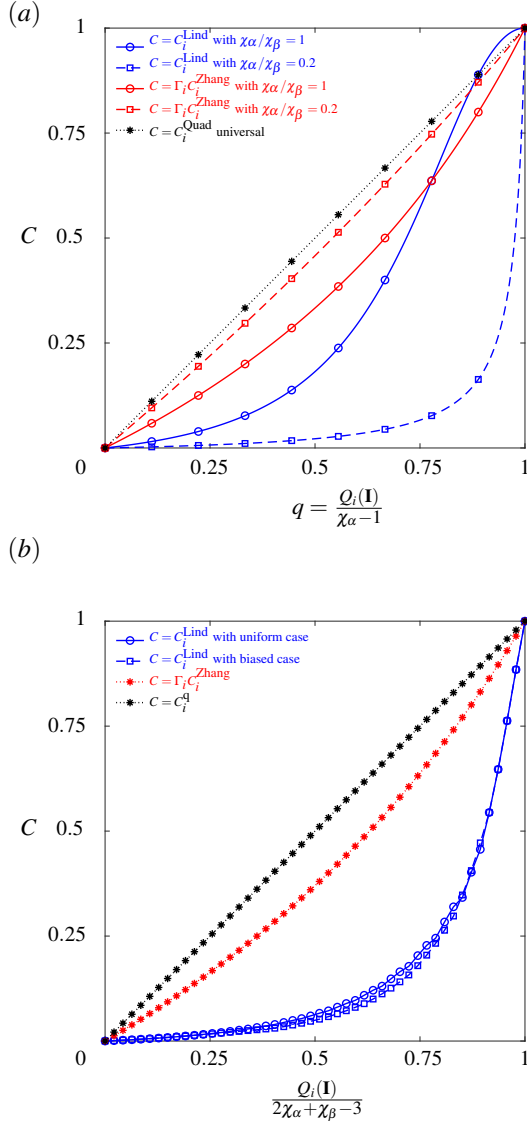


FIG. 3: Comparison among the different clustering coefficients of hypergraphs. The quad clustering coefficient  $C_i^{\text{q}}$ , Lind's clustering coefficient  $C_i^{\text{Lind}}$ , and Zhang's clustering coefficient  $C_i^{\text{Zhang}}$  (markers) are plotted as a function of the number of quads  $Q_i$  incident to a node  $i$  (the scaling factor on the  $x$ -axis is chosen to make the variable's range  $[0, 1]$ ). Upper Panel: node  $i$  has degree  $k_i = 2$  and is connected to two hyperedges  $\alpha$  and  $\beta$ , with cardinalities  $\chi_\alpha = 10$  and  $\chi_\beta$  as indicated in the legend. Lines denote the functions given by Eqs. (21) and (25) for  $C_i^{\text{Lind}}$  and  $C_i^{\text{Zhang}}$ , respectively. Lower Panel: node  $i$  has degree  $k_i = 3$  and interacts with hyperedges  $\alpha$ ,  $\beta$  and  $\gamma$ , of cardinalities  $\chi_\alpha = 15$ ,  $\chi_\beta = 20$ , and  $\chi_\gamma = 25$ , respectively. Circles and squares represent values of  $C^{\text{Lind}}$  for different values of  $q_{i\alpha\beta}$ ,  $q_{i\alpha\gamma}$ ,  $q_{i\beta\gamma}$ , obtained from two different prescriptions, i.e. uniform and biased, as explained in Appendix C). In the lower panel, lines are a guide to the eye.

Taking the limit of large  $N$  while keeping the mean node degree

$$c \equiv \frac{M}{N} \chi \quad (30)$$

fixed, and thus finite, we obtain

$$\langle C_i^{\text{q}}(\mathbf{I}) \rangle_\chi = \frac{\chi - 1}{N} [1 - e^{-c} (1 + c)] + \mathcal{O}\left(\frac{1}{N^2}\right). \quad (31)$$

Note that the average quad clustering coefficient decreases as  $1/N$  with the order of the hypergraph, implying that the density of quads vanishes in the limit of infinitely large, sparse, hypergraphs. For large values of  $\chi$ , but still  $\chi \ll N$ , we get the simple formula

$$\langle C_i^{\text{q}}(\mathbf{I}) \rangle_\chi = \frac{\chi}{N} + \mathcal{O}\left(\frac{1}{N^2}\right) + \mathcal{O}\left(\frac{1}{\chi}\right) \quad (32)$$

stating that the average density of quads equals the cardinality  $\chi$  divided by the number  $N$  of nodes.

## 2. $(c, \chi)$ -regular ensemble

In the  $(c, \chi)$ -regular ensemble the probability assigned to a hypergraph with incidence matrix  $\mathbf{I}$  is defined by

$$P_{c, \chi}(\mathbf{I}) \equiv \frac{1}{\mathcal{N}_{k, \chi}} \prod_{j=1}^N \delta_{c, k_j(\mathbf{I})} \prod_{\alpha=1}^M \delta_{\chi, \chi_\alpha(\mathbf{I})}, \quad (33)$$

where  $\mathcal{N}_{k, \chi} = \sum_{\mathbf{I}} \prod_{j=1}^N \delta_{c, k_j(\mathbf{I})} \prod_{\alpha=1}^M \delta_{\chi, \chi_\alpha(\mathbf{I})}$  is the normalization constant.

In Appendix D 2 we derive the average quad clustering coefficient for this model in the limit  $N \gg 1$  with fixed values of  $c$  and  $\chi$ , and with  $M = (c/\chi)N$ . Neglecting subleading order corrections, we find for the average quad clustering coefficient the expression

$$\langle C_i^{\text{q}}(\mathbf{I}) \rangle_{c, \chi} = \frac{c - 1}{c} \frac{\chi - 1}{N} + \mathcal{O}\left(\frac{1}{N^2}\right). \quad (34)$$

In the limit of large values of  $k$  and  $\chi$ , we recover Eq. (32), indicating that in this limit the average clustering coefficient is independent of the degree distribution. However, at finite  $k$  and  $\chi$  the average clustering coefficient depends on the degree fluctuations, as (34) differs from (31).

## 3. $(\vec{k}, \chi)$ -regular ensemble

In the  $(\vec{k}, \chi)$ -regular ensemble the probability assigned to incidence matrices  $\mathbf{I}$  is given by

$$P_{\vec{k}, \chi}(\mathbf{I}) = \frac{1}{\mathcal{N}_{\vec{k}, \chi}} \prod_{j=1}^N \delta_{\vec{k}, k_j(\mathbf{I})} \prod_{\alpha=1}^M \delta_{\chi, \chi_\alpha(\mathbf{I})}, \quad (35)$$

where  $\mathcal{N}_{k,\chi} = \sum_{\mathbf{I}} \prod_{j=1}^N \delta_{k_j,k_j(\mathbf{I})} \prod_{\alpha=1}^M \delta_{\chi,\chi_\alpha(\mathbf{I})}$  is the normalization constant.

Neglecting subleading order terms, the average quad clustering coefficient is given by (see Appendix D 2)

$$\begin{aligned} \langle C_i^q(\mathbf{I}) \rangle_{\bar{k},\chi} & \\ &= \frac{\chi-1}{\bar{k}^2 N} \overline{k(k-1)} (1 - p_{\text{deg}}(0) - p_{\text{deg}}(1)) + \mathcal{O}\left(\frac{1}{N^2}\right) \end{aligned} \quad (36)$$

where the overline denotes the mean value

$$\overline{f(k)} \equiv \sum_{k=0}^{\infty} p_{\text{deg}}(k) f(k), \quad (37)$$

with

$$p_{\text{deg}}(k) \equiv \lim_{N \rightarrow \infty} \frac{\sum_{j=1}^N \delta_{k,k_j}}{N} \quad (38)$$

and  $f(k)$  is an arbitrary real-valued function defined on  $k \in \mathbb{N} \cup \{0\}$ . Using  $p_{\text{deg}}(k) = \delta_{k,c}$  and  $p_{\text{deg}}(k) = e^{-c} c^k / k!$  in Eq. (36), we find, respectively, the Eqs. (34) and (31). Hence, the formula (36) generalises Eqs. (34) and (31).

Notice that the first term in Eq. (36) diverges when the degree distribution  $p_{\text{deg}}(k)$  has a diverging second moment, indicating that the average clustering coefficient of random hypergraphs with diverging second moments decreases slower than  $1/N$  as a function of  $N$ . This result is compatible with what is known for random graphs, as the average number of cycles of finite length diverges with the second moment of the degree distribution (see Equation (9) in Ref.<sup>23</sup>).

## B. Biregular cardinalities

Having studied in detail the case with regular cardinalities, including the effect of degree fluctuations, we now analyze how fluctuations in the cardinality affect the average quad clustering coefficient. We focus on the simplest case of biregular ensembles, where  $M_1$  hyperedges have cardinality  $\chi_1$  and the remaining  $M - M_1$  have cardinality  $\chi_2$ . In this case, the probability of incidence matrices  $\mathbf{I} \in \{0, 1\}^{NM}$  takes the form

$$P_{\chi_1,\chi_2}(\mathbf{I}) = \frac{1}{\mathcal{N}_{\chi_1,\chi_2}} \prod_{\alpha=1}^{M_1} \delta_{\chi_1,\chi_\alpha(\mathbf{I})} \prod_{\beta=M_1+1}^M \delta_{\chi_2,\chi_\beta(\mathbf{I})}, \quad (39)$$

where as before  $\mathcal{N}_{\chi_1,\chi_2}$  is the normalisation constant.

In Appendix E, we show that the average clustering coefficient, defined by

$$\langle C_i^q(\mathbf{I}) \rangle_{\chi_1,\chi_2} \equiv \sum_{\mathbf{I}} C_i^q(\mathbf{I}) P_{\chi_1,\chi_2}(\mathbf{I}), \quad (40)$$

is given by

$$\begin{aligned} \langle C_i^q(\mathbf{I}) \rangle_{\chi_1,\chi_2} &= \sum_{u=2}^{M_1} \sum_{v=0}^{M_2} \frac{\Lambda_{2,0}(u,v)}{\Phi(u,v)} \\ &+ \sum_{u=1}^{M_1} \sum_{v=1}^{M_2} \frac{\Lambda_{1,1}(u,v)}{\Phi(u,v)} + \sum_{u=0}^{M_1} \sum_{v=2}^{M_2} \frac{\Lambda_{0,2}(u,v)}{\Phi(u,v)} \end{aligned} \quad (41)$$

where  $M_2 = M - M_1$  and we introduced the functions

$$\begin{aligned} \Lambda_{a,b}(u,v) &\equiv 2(N-1) \binom{M_1}{a} \binom{M_2}{b} \\ &\times \left[ \binom{N-2}{\chi_1-2} \right]^a \left[ \binom{N-2}{\chi_2-2} \right]^b \\ &\times \binom{M_1-a}{u-a} \left[ \binom{N-1}{\chi_1-1} \right]^{u-a} \left[ \binom{N-1}{\chi_1} \right]^{M_1-u} \\ &\times \binom{M_2-b}{v-b} \left[ \binom{N-1}{\chi_2-1} \right]^{v-b} \left[ \binom{N-1}{\chi_2} \right]^{M_2-v}, \end{aligned} \quad (42)$$

and

$$\begin{aligned} \Phi(u,v) &\equiv \binom{N}{\chi_1}^{M_1} \binom{N}{\chi_2}^{M_2} [(\chi_1-1)(u+v)(u+v-1) \\ &+ v(\chi_2-\chi_1)(v-1)]. \end{aligned} \quad (43)$$

We have not been able to simplify the expression (41)-(43) further, not even in the sparse limit. Hence, although models with degree fluctuations are analytical tractable, as shown in Sec. IV A 3, it is significantly more difficult to deal with models with heterogeneous cardinalities.

Setting  $\chi_1 = \chi_2 = \chi$  in Eq. (41), we find the Eq. (29). Hence, the formula (41) generalises Eq. (29).

We understand each term in Eq. (41) as follows: the first and last terms consider quads consisting of two hyperedges with the same cardinality, and the middle term considers the case where the two hyperedges have different cardinalities.

## V. QUAD CLUSTERING COEFFICIENT IN REAL WORLD HYPERGRAPHS

Having established a theoretical understanding of quad clustering coefficients in random hypergraphs, we focus now our attention on the quad clustering coefficient in real-world hypergraphs. To this aim, we build hypergraphs out of six datasets, which are related to Github, Youtube, NDC-substances, food recipes, Walmart, and crime involvement. As detailed in Table I, the real-world hypergraphs have diverse topologies: their order ranges from  $N \approx 10^3$  to  $N \approx 10^5$ , their mean degree ranges from  $\bar{k} \approx 3$  to  $\bar{k} \approx 60$ , and their mean cardinality ranges from  $\bar{\chi} \approx 3$  to  $\bar{\chi} \approx 10$  [see Appendix F for more detailed information about these data sets].

### A. Mean quad clustering coefficient

The mean quad clustering coefficient

$$\bar{C}^q(\mathbf{I}) \equiv \frac{1}{N} \sum_{i=1}^N C_i^q(\mathbf{I}) \quad (44)$$

is a real number  $\bar{C}^q(\mathbf{I}) \in [0, 1]$  that quantifies the density of quads in the hypergraph represented by  $\mathbf{I}$ . In Figure 4, we compare the mean clustering coefficients  $\bar{C}^q(\mathbf{I}_{\text{real}})$  for the six

TABLE I: Characteristics of the real-world hypergraphs considered in this Paper: number of nodes  $N$  and hyperedges  $M$ , mean degree  $\bar{k}$  and mean cardinality  $\bar{\chi}$ , mean quad clustering coefficient  $\bar{C}^q(\mathbf{I}_{\text{real}})$ , mean Lind's clustering coefficient  $\bar{C}^{\text{Lind}}(\mathbf{I}_{\text{real}})$ , mean Zhang's clustering coefficient  $\bar{C}^{\text{Zhang}}(\mathbf{I}_{\text{real}})$ , the average mean quad clustering coefficient  $\langle \bar{C}^q(\mathbf{I}) \rangle$ , the average mean Lind's clustering coefficient  $\langle \bar{C}^{\text{Lind}}(\mathbf{I}) \rangle$  and the average mean Zhang's clustering coefficient  $\langle \bar{C}^{\text{Zhang}}(\mathbf{I}) \rangle$  of the corresponding configuration model with fixed degree sequence  $\bar{k}(\mathbf{I}_{\text{real}})$  and cardinality sequence  $\bar{\chi}(\mathbf{I}_{\text{real}})$ . For more details see Appendix F.

| Dataset           | $N$    | $M$     | $\bar{k}$ | $\bar{\chi}$ | $\bar{C}^q(\mathbf{I}_{\text{real}})$ | $\bar{C}^{\text{Lind}}(\mathbf{I}_{\text{real}})$ | $\bar{C}^{\text{Zhang}}(\mathbf{I}_{\text{real}})$ | $\langle \bar{C}^q(\mathbf{I}) \rangle$ | $\langle \bar{C}^{\text{Lind}}(\mathbf{I}) \rangle$ | $\langle \bar{C}^{\text{Zhang}}(\mathbf{I}) \rangle$ |
|-------------------|--------|---------|-----------|--------------|---------------------------------------|---|--|---|---|--|
| NDC-substances    | 5,556  | 112,919 | 12.2      | 2.0          | 0.2760                                | 0.1418  | 0.1792   | 0.0252                                  | 0.0012  | 0.0093   |
| Youtube           | 94,238 | 30,087  | 3.1       | 9.8          | 0.0920                                | 0.0094  | 0.0225   | 0.0142                                  | 0.0001  | 0.0043   |
| Food recipe       | 6,714  | 39,774  | 63.8      | 10.8         | 0.1118                                | 0.0178  | 0.0501   | 0.0658                                  | 0.0054  | 0.0271   |
| Github            | 56,519 | 120,867 | 7.8       | 3.6          | 0.1129                                | 0.0408  | 0.0329   | 0.0084                                  | 0.0001  | 0.0029   |
| Crime involvement | 829    | 551     | 1.8       | 2.7          | 0.0369                                | 0.0243  | 0.0169   | 0.0037                                  | 0.0010  | 0.0013   |
| Walmart           | 88,860 | 69,906  | 5.2       | 6.6          | 0.0120                                | 0.0046  | 0.0046   | 0.0010                                  | 0.0001  | 0.0003   |

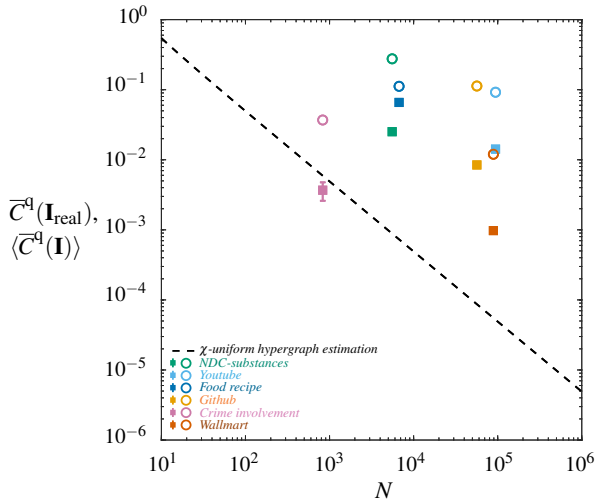


FIG. 4: Comparison between mean, quad clustering coefficients  $\bar{C}^q(\mathbf{I}_{\text{real}})$  (unfilled, circles) in real-world hypergraphs, and average, mean clustering coefficients  $\langle \bar{C}^q(\mathbf{I}) \rangle$  (filled, squares) in random hypergraphs with prescribed degree and cardinality sequences  $\bar{k}(\mathbf{I}_{\text{real}})$  and  $\bar{\chi}(\mathbf{I}_{\text{real}})$ . Estimates of  $\langle \bar{C}^q(\mathbf{I}) \rangle$  are based on 100 hypergraph realisations, and error bars show the error on the mean, whenever they are larger than the marker size. The dashed line represents the prediction Eq. (31) for  $\chi$ -regular hypergraphs with  $\chi = 5.9$  and  $c = 20/\chi$ , which are, respectively, the average cardinality and mean degree of all hyperedges and nodes in all real-world datasets.

canonical hypergraphs under study, represented by  $\mathbf{I}_{\text{real}}$ , with those of the configuration model<sup>24</sup> with a prescribed degree sequence  $\bar{k}(\mathbf{I}_{\text{real}})$  and cardinality sequence  $\bar{\chi}(\mathbf{I}_{\text{real}})$  (see Appendix G for a description of the algorithm used to generate hypergraphs from the configuration model). The results in Fig. 4 reveal that the quad clustering coefficients of real-world networks are significantly larger than the average clustering coefficient  $\langle \bar{C}^q(\mathbf{I}) \rangle$  of the corresponding configuration models ( $\langle \bar{C}^q(\mathbf{I}) \rangle \approx 0.10 \bar{C}^q(\mathbf{I}_{\text{real}})$ , see Table I). Hence, the density of quads in real-world networks is higher than what is ex-

pected in the configuration model, similarly to previous findings for clustering coefficients in networks with pairwise interactions, see, e.g., Ref.<sup>2</sup>. Similar conclusions can be drawn from comparing Lind's and Zhang's clustering coefficients between real-world and random networks (see Table I). However, the corresponding values of Lind's and Zhang's clustering coefficients are one order of magnitude smaller than the quad clustering coefficient, consistent with the behaviour of the clustering coefficients as a function of the number of quads as shown in Fig. 3 and discussed in Sec. III.

## B. Distribution of quad clustering coefficients

As real-world hypergraphs exhibit a larger number of quads than expected from random models, we investigate the fluctuations in the quad clustering coefficient. We quantify the fluctuations of the quad clustering coefficient by its distribution

$$P(C^q; \mathbf{I}) \equiv \frac{1}{N} \sum_{i=1}^N \delta(C^q - C_i^q(\mathbf{I})). \quad (45)$$

Figure 5 shows the distribution  $P(C^q; \mathbf{I}_{\text{real}})$  for the six real-world hypergraphs under study. We highlight a few noteworthy features of these plots. Firstly, a significant proportion of nodes possess a near zero quad clustering coefficient, viz., between 50-70 % in the Hypergraphs (a)-(d) and over 90% in the Hypergraphs (e)-(f). Secondly, for the remaining nodes the distribution of  $C_i^q$  is broad. This latter feature stands in contrast with the average distribution  $\langle P(C^q; \mathbf{I}) \rangle$  in the corresponding configuration model with prescribed degree sequence  $\bar{k}(\mathbf{I}_{\text{real}})$  and cardinality sequence  $\bar{\chi}(\mathbf{I}_{\text{real}})$ , generated by a standard stub-joining algorithm<sup>25</sup>, also plotted in Fig. 5. Thirdly, the hypergraphs in Fig. 5 exhibit a peak at  $C^q \approx 1$ , which is most clearly visible in the NDC-substances hypergraph (a) and the Github hypergraph (hypergraph (d)).

As discussed in Sec. III, quad clustering can also be quantified with the Lind and Zhang clustering coefficients. As shown in Fig. 6, the peak at  $C^q \approx 1$  also appears when quantifying quad clustering with the Lind clustering coefficient or the Zhang clustering. However, the distributions  $P(C^{\text{Lind}}; \mathbf{I}_{\text{real}})$



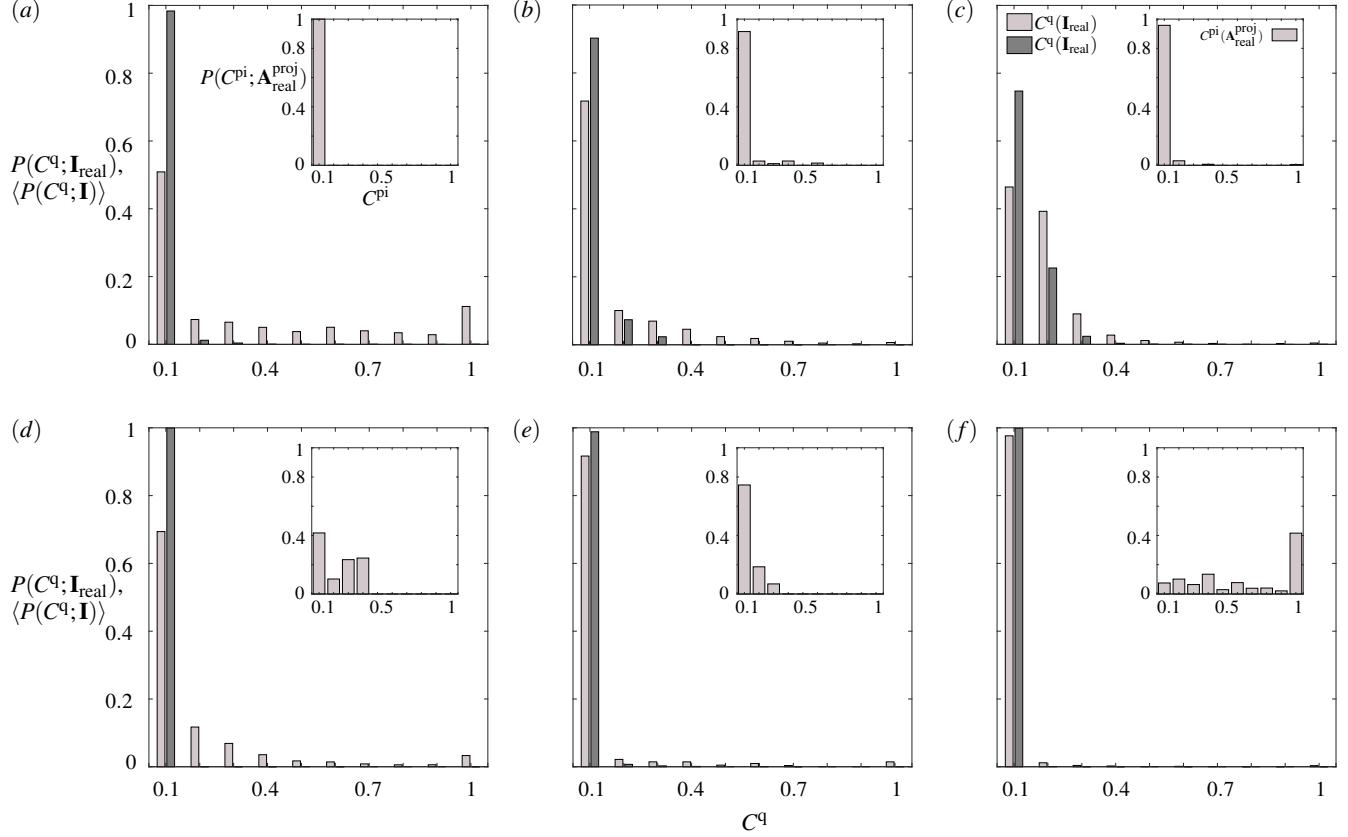


FIG. 5: *Distribution of quad clustering coefficients in nondirected hypergraphs.* Comparison between the distributions  $P(C^q; \mathbf{I}_{\text{real}})$  of quad clustering coefficients in real-world hypergraphs (light grey histograms) and the average distribution  $\langle P(C^q; \mathbf{I}) \rangle$  (dark grey histograms) of the corresponding configuration model with a prescribed degree sequence  $\bar{k}(\mathbf{I}_{\text{real}})$  and cardinality sequence  $\bar{\chi}(\mathbf{I}_{\text{real}})$ . The estimate of  $\langle P(C^q; \mathbf{I}) \rangle$  has been obtained from 100 graph realisations. The inset shows the distribution  $P(C^{\text{pi}}; \mathbf{A}_{\text{real}}^{\text{proj}})$  of pairwise clustering coefficients in the projected network  $\mathbf{A}_{\text{real}}^{\text{proj}}$  formed from pairwise interactions obtained with the formula (10). Note that the distributions  $P(C^q; \mathbf{I}_{\text{real}})$  show a peak at  $C^q = 1$ , while the distributions  $P(C^{\text{pi}}; \mathbf{A}_{\text{real}}^{\text{proj}})$  do not show a peak at  $C^{\text{pi}} = 1$  [except for Hypergraph (f)]. The real-world hypergraphs considered are: (a) *NDC-substances*, (b) *Youtube*, (c) *Food recipe*, (d) *Github*, (e) *Crime involvement* and (f) *Walmart*; see Table I.

and  $P(C^{\text{Zhang}}; \mathbf{I}_{\text{real}})$  have a larger peak at the origin, while the number of nodes with an intermediate value (not zero or one) is smaller. This result is consistent with the nonlinearity observed in Fig. 3. Indeed, since the  $C^{\text{Lind}}$  and  $C^{\text{Zhang}}$  clustering coefficients are nonlinear, nodes accumulate at values  $C^{\text{Lind}} \approx 0, 1$  and  $C^{\text{Zhang}} \approx 0, 1$ , and hence these clustering coefficients are less effective at discriminating nodes based on their density of quads.

Importantly, disregarding for now Hypergraph (f) on which we come back later, the peak at  $C^q(\mathbf{I}) \approx 1$  peak is not captured by the pairwise clustering coefficient evaluated on the corresponding projected graphs represented by  $\mathbf{A}^{\text{proj}}$ . Indeed, as shown in the inset of Figure 5, the

$$P(C^{\text{pi}}; \mathbf{A}^{\text{proj}}) \equiv \frac{1}{N} \sum_{i=1}^N \delta(C^{\text{pi}} - C_i^{\text{pi}}(\mathbf{A}^{\text{proj}})) \quad (46)$$

where  $\mathbf{A}^{\text{proj}}$  is the adjacency matrix of the projected graph as defined in (10), does not exhibit a peak at large values. Hence quad clustering captures a characteristic distinct to hypergraphs and that is not captured by pairwise clustering coefficients.

As shown in Fig. 5, Hypergraph (f), exhibits clustering properties that are different from those of the other networks. Specifically, Hypergraph (f) exhibits a peak at 1 in the distribution of quad clustering coefficients, and does not have a peak at 1 observed in the distribution of pairwise clustering coefficients of the projected graph. To understand this peculiar property of Hypergraph (f), we examine the network motifs formed by the nodes  $i$  for which it holds that both  $C_i^q < 0.5$  and  $C_i^{\text{pi}} > 0.8$  (a total of 38,520 nodes out of the 88,860 satisfy this condition). We have found two type of structures among such nodes: In particular, 75% of the nodes have  $\sum_{\chi=3}^{\infty} k_i(\mathbf{I}; \chi) = 1$ , and hence their quad clustering co-

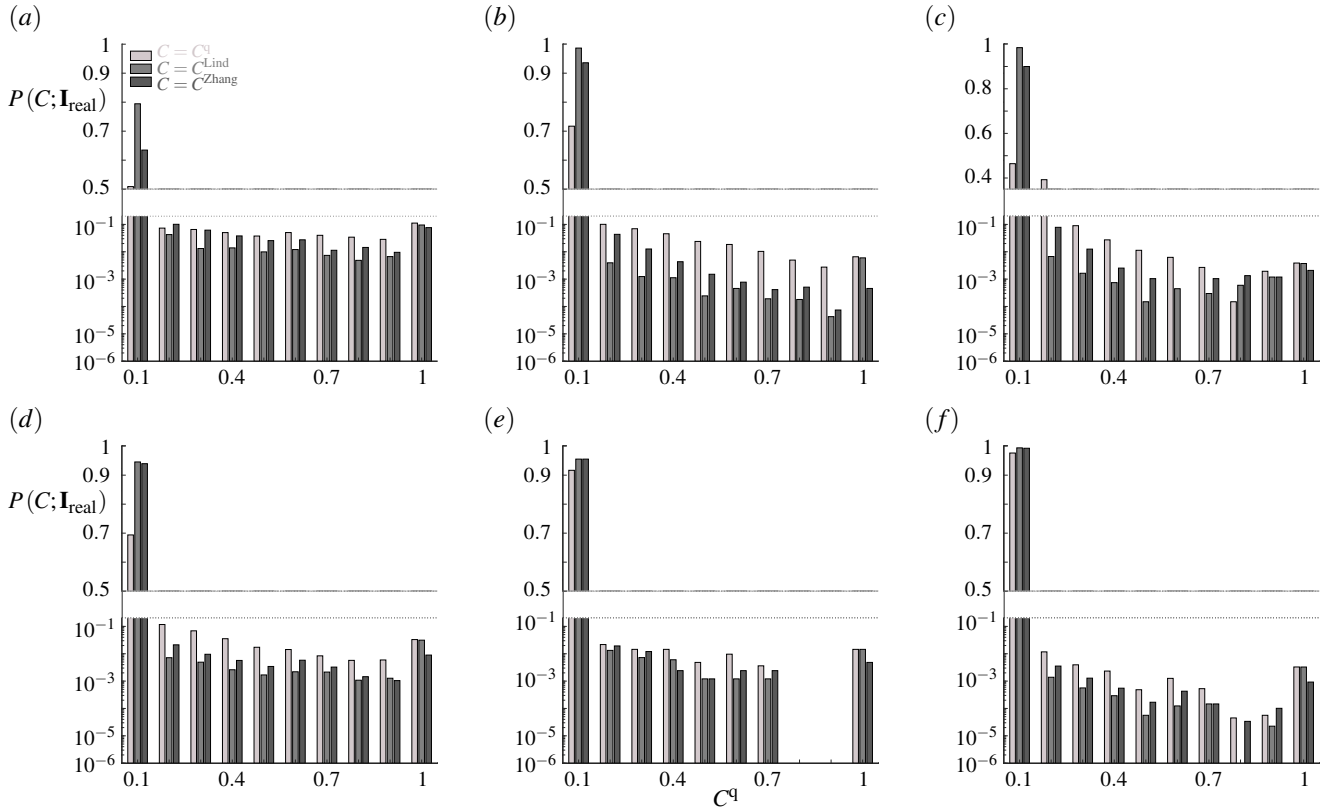


FIG. 6: Comparison of distributions of three clustering coefficients examined in the real-world hypergraphs. The light grey histograms represent the distributions of the quad clustering coefficient  $P(C^q; \mathbf{I}_{\text{real}})$ . The grey bar graphs show the distributions of Lind's clustering coefficient  $P(C^{\text{Lind}}; \mathbf{I}_{\text{real}})$ . And the dark grey histograms denote the distributions of Zhang's clustering coefficient  $P(C^{\text{Zhang}}; \mathbf{I}_{\text{real}})$ . Panels represent different real-world hypergraphs, as explained in the caption of Fig. 5. Note the discontinuous scale on the y-axis, with a linear scale for  $y > 0.5$  and a logarithmic scale for  $y < 0.5$ .

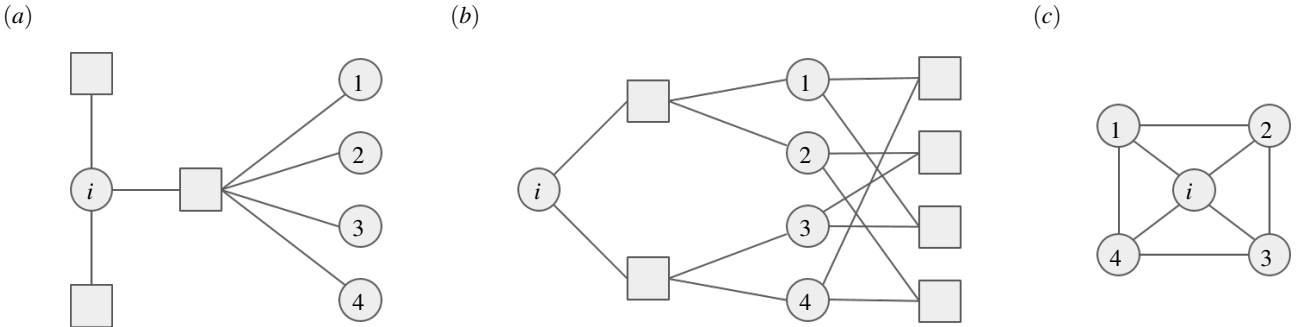


FIG. 7: Illustration of motifs in the Walmart network (Hypergraph (f)) centered around nodes  $i$  for which both  $C_i^q = 0$  and  $C_i^{\text{pi}} = 1$ . Panel (a): motif with degree  $\sum_{\chi=3}^{\infty} k_i(\mathbf{I}; \chi) = 1$ ; Panel (b): motif with degree  $k_i^* > 1$ , but nevertheless  $C_i^q = 0$  and  $C_i^{\text{pi}} = 1$ ; Panel (c): projected graph for the networks illustrated in Panels (a) and (b), yielding  $C_i^{\text{pi}} = 1$ .

efficient equals zero and their pairwise clustering coefficient equals one; see Fig. 7(a) for an illustration of such a motif. The remaining 25% of the nodes have a structure similar to those in Fig. 7(b): the neighbourhoods of the hyperedges incident to the central node are disjoint when we exclude the central node. However, each pair of nodes  $j_1, j_2$  that are incident to hyperedges incident to the central node, are themselves directly connected by a hyperedge. Consequently, also in this

case  $C_i^q = 0$  and  $C_i^{\text{pi}} = 1$ . Note that in the real-world examples, the latter motifs are slightly different from those shown in Fig. 7(b), and hence values of  $C_i^q \in [0, 0.5]$  and  $C_i^{\text{pi}} \in [0.8, 1]$  are observed.

### C. Quad clustering coefficients as a function of degree and cardinality

In this Subsection, we make a study of the topological properties of nodes that have a large quad clustering coefficient  $C_i^q \approx 1$ .

First, we address the correlations between  $C_i^q(\mathbf{I}_{\text{real}})$  and the modified degree  $k_i^*(\mathbf{I}_{\text{real}})$ , as defined in Eq. (7). We consider the modified degree  $k_i^*$  instead of the degree  $k_i$ , as by default hyperedges with unit cardinality do not contribute to the quad clustering coefficient. In Fig. 8 we present scatter plots containing all the pairs  $(k_i^*(\mathbf{I}_{\text{real}}), C_i^q(\mathbf{I}_{\text{real}}))$  for the six canonical real-world hypergraphs that we consider in this Paper, one marker for each node in the hypergraph. The red dashed line is a fit to the scaling relation  $C^q \sim (k^*)^{-\beta}$  and it shows the decreasing trend of the quad clustering with the modified degrees. This demonstrates that highly clustered nodes have on average lower degrees than nodes with small quad clustering coefficients. Nevertheless, up to modified degrees  $k_i^* \approx 100$  there exist nodes with  $C_i^q(\mathbf{I}) \approx 1$ , and hence real-world hypergraphs contain highly clustered nodes that have large degrees. This result is surprising, as the denominator of the quad clustering coefficient increases fast as a function of  $k_i$ , see Eqs. (13) and (17), hence one may have expected that the highly clustered nodes with  $C_i^q(\mathbf{I}) \approx 1$  consist exclusively of nodes with small modified degrees.

This results is confirmed by Fig. 9 that compares the distribution

$$P(k^*; \mathbf{I}) \equiv \frac{1}{N} \sum_{i=1}^N \delta_{k^*, k_i^*}(\mathbf{I}) \quad (47)$$

of the modified degrees  $k_i^*$  sampled uniformly from the set  $\mathcal{V}$  of hypergraph nodes with the distribution

$$P(k^* | C^q = 1; \mathbf{I}) \equiv \frac{\sum_{i=1}^N \delta_{k^*, k_i^*}(\mathbf{I}) \delta_{C_i^q(\mathbf{I}), 1}}{\sum_{i=1}^N \delta_{C_i^q(\mathbf{I}), 1}} \quad (48)$$

of nodes that have a clustering coefficient equal to one. As expected, the modified degree of highly clustered nodes with  $C_i^q = 1$  are concentrated on small values of the modified degrees. Surprisingly, however, in the real-world hypergraphs (a), (d) and (f), highly clustered nodes can have modified degrees as large as  $k_i^* \approx 100$ . As an illustration, for the *NDC-substances* network, Fig. 9(a), the maximum value of  $k_i^*$  amongst nodes with  $C^q = 1$  is  $k_i^* = 192$ . This is unexpectedly large, as it implies that the 192 hyperedges connected to node  $i$  form a fully clustered configuration.

To further describe the topological properties of the neighbourhood sets of highly clustered nodes, we analyse the cardinalities of the hyperedges that are incident to a highly clustered node. We expect that strongly clustered nodes ( $C_i^q(\mathbf{I}) \approx 1$ ) have neighbouring nodes with small cardinalities, as the denominator in the quad clustering coefficient increases fast as a function of the cardinalities of the neighbouring nodes. To quantify fluctuations in the cardinalities of hyperedges, we

define the joint distribution

$$W(k, \chi; \mathbf{I}) \equiv \frac{\sum_{i=1}^N \sum_{\alpha=1}^M I_{i\alpha} \delta_{k, k_i(\mathbf{I})} \delta_{\chi, \chi_\alpha(\mathbf{I})}}{\sum_{i=1}^N \sum_{\alpha=1}^M I_{i\alpha}}, \quad (49)$$

of degrees and cardinalities of randomly selected links connecting nodes with hyperedges. Its marginal distribution

$$W^*(\chi; \mathbf{I}) = \frac{\sum_{k=1}^M W(k, \chi; \mathbf{I})}{\sum_{k=1}^M \sum_{\chi=2}^{N-1} W(k, \chi; \mathbf{I})}, \quad (50)$$

quantifies the fluctuations of the cardinalities of hyperedges at the end point of a randomly selected link, and excluding nodes with cardinality one.

In Fig. 10, we compare the distribution  $W^*(\chi; \mathbf{I})$  with the related distribution  $W^*(\chi | C^q = 1; \mathbf{I})$  defined on nodes with a quad clustering coefficient equal to one. The latter distribution is defined by

$$W^*(\chi | C^q = 1; \mathbf{I}) = \frac{\sum_{k=1}^M W(k, \chi | C^q = 1; \mathbf{I})}{\sum_{k=1}^M \sum_{\chi=2}^{N-1} W(k, \chi | C^q = 1; \mathbf{I})}, \quad (51)$$

where

$$W(k, \chi | C^q = 1; \mathbf{I}) \equiv \frac{\sum_{i=1}^N \sum_{\alpha=1}^M \delta_{C_i^q(\mathbf{I}), 1} I_{i\alpha} \delta_{k, k_i(\mathbf{I})} \delta_{\chi, \chi_\alpha(\mathbf{I})}}{\sum_{i=1}^N \sum_{\alpha=1}^M \delta_{C_i^q(\mathbf{I}), 1} I_{i\alpha}}. \quad (52)$$

Interestingly, Fig. 10 reveals that nodes with  $C_i^q(\mathbf{I}) = 1$  can have a large cardinality  $\chi \approx 2000$ . This highlights that the neighbourhood sets of highly clustered nodes can have a large number of quads, as they contain hyperedges with large cardinality. Comparing Figs. 9 and 10, we observe that support of the distribution  $W^*(\chi; \mathbf{I}_{\text{real}})$  is in most cases equal to the support of  $W^*(\chi | C^q = 1)$ , while the support of the distribution  $P(k^*; \mathbf{I}_{\text{real}})$  is significantly smaller than the support of  $P(k^* | C^q = 1)$ . Hence, highly clustered neighbourhoods are more biased towards low degree nodes than towards nodes of low cardinality, which is consistent with the formula (17) for the maximal number of quads a node can have.

## VI. QUAD CLUSTERING COEFFICIENT FOR DIRECTED HYPERGRAPHS

In this Section we define a quad clustering coefficient for directed hypergraphs and we analyse its properties in real-world directed hypergraphs.

### A. Preliminaries on directed hypergraphs

A directed hypergraph is a quadruplet  $\mathcal{H}^{\leftrightarrow} = (\mathcal{V}, \mathcal{W}, \mathcal{E}^{\text{in}}, \mathcal{E}^{\text{out}})$  consisting of the set  $\mathcal{V}$  of  $N = |\mathcal{V}|$  nodes, the set  $\mathcal{W}$  of  $M = |\mathcal{W}|$  hyperedges, and the sets  $\mathcal{E}^{\text{in}} \subset \mathcal{V} \times \mathcal{W}$  and  $\mathcal{E}^{\text{out}} \subset \mathcal{V} \times \mathcal{W}$  of directed inlinks and outlinks, respectively. Both inlinks and outlinks consist of pairs  $(i, \alpha)$  with  $i \in \mathcal{V}$  and  $\alpha \in \mathcal{W}$ , albeit the former represents

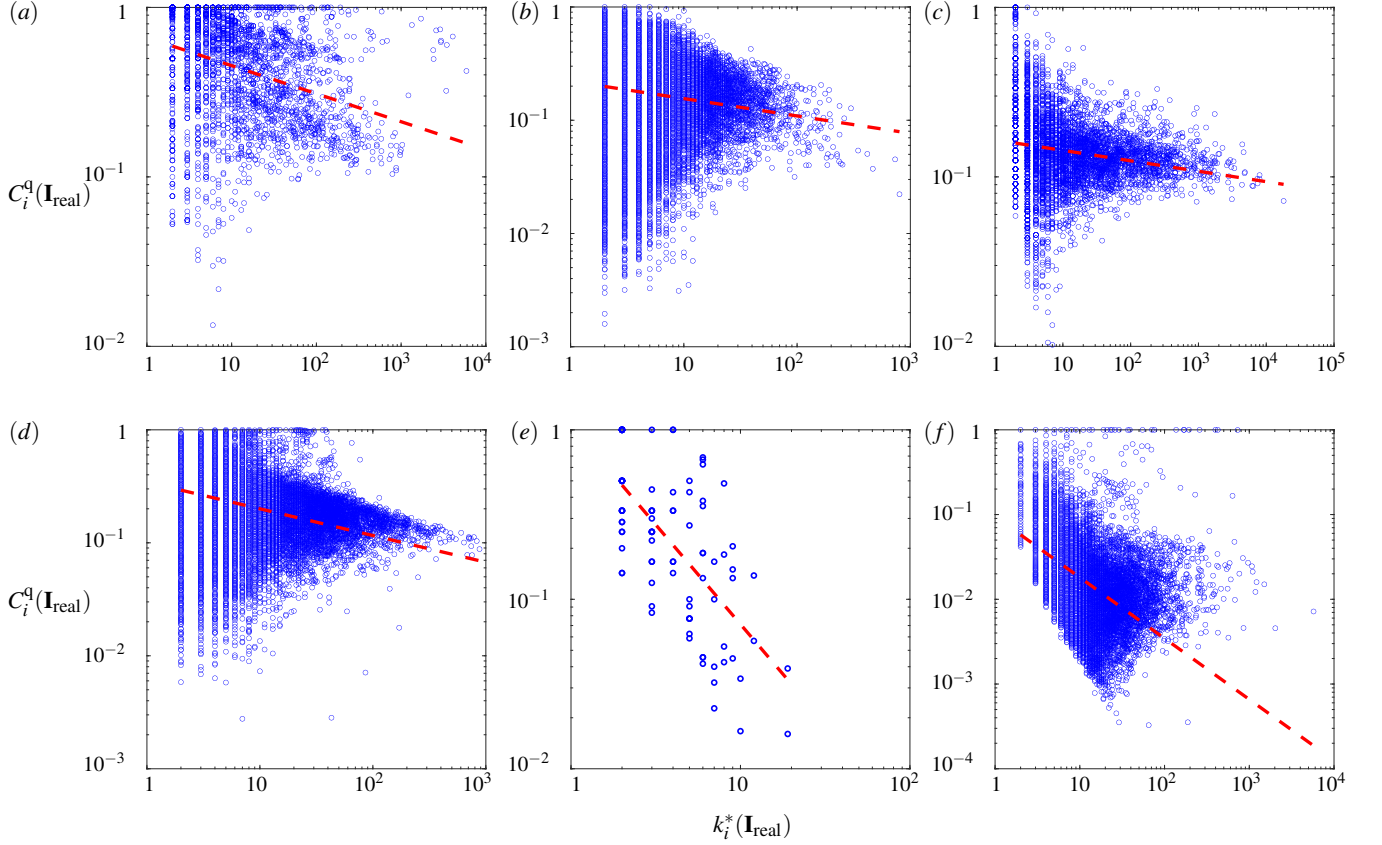


FIG. 8: Scatter plots constructed from the pairs  $(k_i^*(\mathbf{I}_{\text{real}}), C_i^q(\mathbf{I}_{\text{real}}))$  of all nodes  $i \in \mathcal{V}(\mathbf{I}_{\text{real}})$  in the canonical, real-world hypergraphs. The lines are a fit to  $C^q \sim (k^*)^{-\beta}$  with the fitted values for  $\beta$  and their 95% confidence intervals equal to  $0.17 \pm 0.01$  (a),  $0.15 \pm 0.01$  (b),  $0.06 \pm 0.01$  (c),  $0.24 \pm 0.01$  (d),  $1.2 \pm 0.2$  (e), and  $0.72 \pm 0.02$  (f). Panels represent different real-world hypergraphs, as explained in the caption of Fig. 5.

links directed from a hyperedge to a vertex, while the latter represents links directed from a vertex to a hyperedge.

We represent simple, directed, hypergraphs with a pair of incidence matrices  $\mathbf{I}^{\leftrightarrow} \equiv (\mathbf{I}^{\rightarrow}, \mathbf{I}^{\leftarrow})$  defined by

$$[\mathbf{I}^{\rightarrow}]_{i\alpha} \equiv \begin{cases} 1 & \text{if } (i, \alpha) \in \mathcal{E}^{\text{out}}, \\ 0 & \text{if } (i, \alpha) \notin \mathcal{E}^{\text{out}} \end{cases} \quad (53)$$

and

$$[\mathbf{I}^{\leftarrow}]_{i\alpha} \equiv \begin{cases} 1 & \text{if } (i, \alpha) \in \mathcal{E}^{\text{in}}, \\ 0 & \text{if } (i, \alpha) \notin \mathcal{E}^{\text{in}}. \end{cases} \quad (54)$$

Figure 11 illustrates different ways of representing hypergraphs with an example.

The *out-degree* and *in-degree* of node  $i \in \mathcal{V}$  are defined by

$$k_i^{\text{out}}(\mathbf{I}^{\rightarrow}) \equiv \sum_{\alpha=1}^M I_{i\alpha}^{\rightarrow} \quad \text{and} \quad k_i^{\text{in}}(\mathbf{I}^{\leftarrow}) \equiv \sum_{\alpha=1}^M I_{i\alpha}^{\leftarrow}, \quad (55)$$

and we also use the notations

$$\vec{k}^{\text{in}}(\mathbf{I}^{\leftarrow}) \equiv (k_1^{\text{in}}(\mathbf{I}^{\leftarrow}), k_2^{\text{in}}(\mathbf{I}^{\leftarrow}), \dots, k_N^{\text{in}}(\mathbf{I}^{\leftarrow})) \quad (56)$$

and

$$\vec{k}^{\text{out}}(\mathbf{I}^{\rightarrow}) \equiv (k_1^{\text{out}}(\mathbf{I}^{\rightarrow}), k_2^{\text{out}}(\mathbf{I}^{\rightarrow}), \dots, k_N^{\text{out}}(\mathbf{I}^{\rightarrow})) \quad (57)$$

for their sequences. Analogously, we define the *out-cardinality* and *in-cardinality* of hyperedge  $\alpha \in \mathcal{H}$  by

$$\chi_{\alpha}^{\text{out}}(\mathbf{I}^{\leftarrow}) \equiv \sum_{i=1}^N I_{i\alpha}^{\leftarrow} \quad \text{and} \quad \chi_{\alpha}^{\text{in}}(\mathbf{I}^{\rightarrow}) \equiv \sum_{i=1}^N I_{i\alpha}^{\rightarrow}, \quad (58)$$

and we also use the corresponding sequences  $\vec{\chi}^{\text{in}}(\mathbf{I}^{\rightarrow})$  and  $\vec{\chi}^{\text{out}}(\mathbf{I}^{\leftarrow})$ . In addition, we define the *modified out- and in-cardinalities*

$$\chi_{\alpha,i}^{\text{out}}(\mathbf{I}^{\leftarrow}) \equiv \sum_{\substack{j=1; \\ j \neq i}}^N I_{j\alpha}^{\leftarrow} \quad \text{and} \quad \chi_{\alpha,i}^{\text{in}}(\mathbf{I}^{\rightarrow}) \equiv \sum_{\substack{j=1; \\ j \neq i}}^N I_{j\alpha}^{\rightarrow} \quad (59)$$

excluding the stubs used to connect to a given node  $i$ .

Lastly, we define the set of hyperedges incident to the node  $i$  as the union

$$\partial_i(\mathbf{I}^{\leftrightarrow}) \equiv \partial_i^{\text{out}}(\mathbf{I}^{\rightarrow}) \cup \partial_i^{\text{in}}(\mathbf{I}^{\leftarrow}) \quad (60)$$

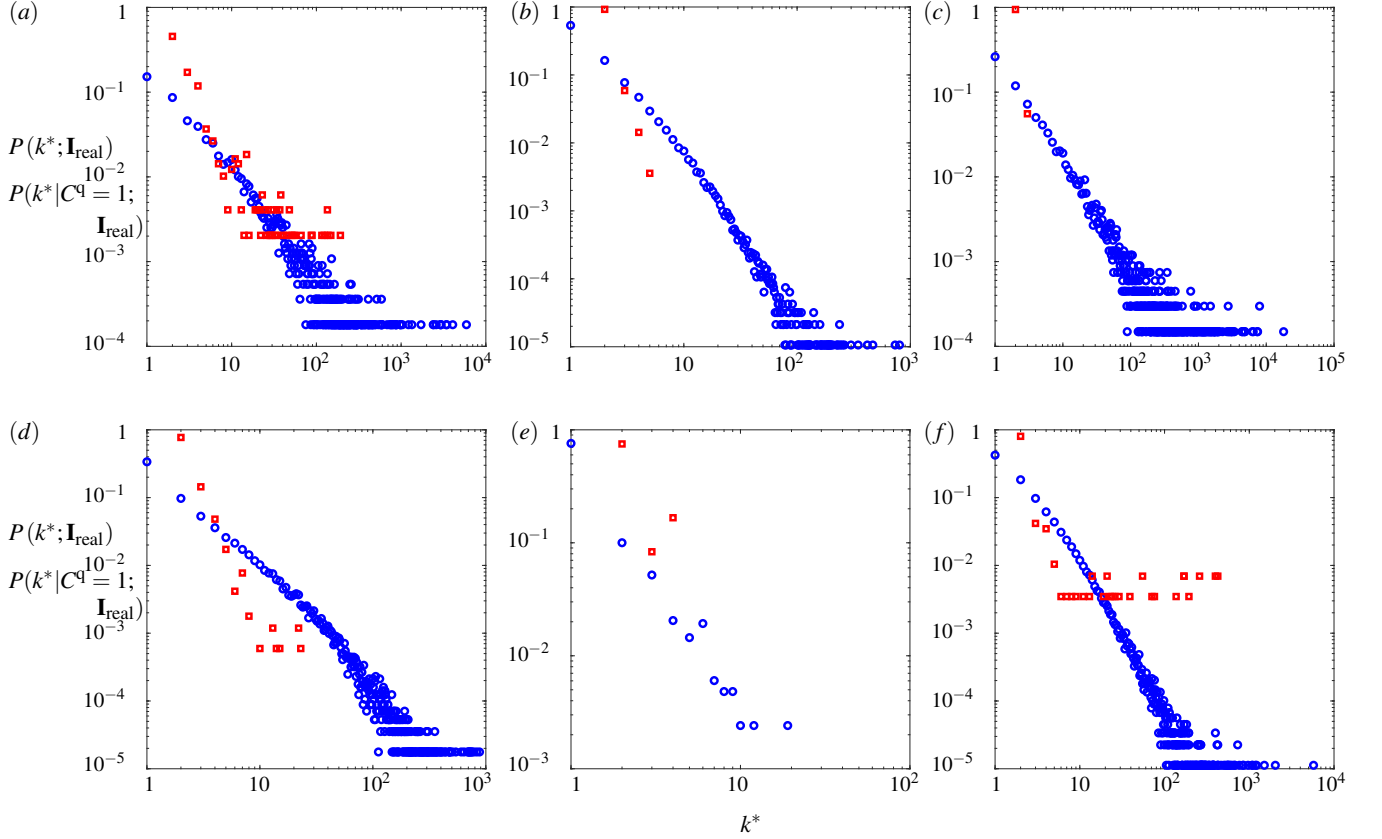


FIG. 9: Distributions of degrees of highly clustered nodes in real-world hypergraphs, and comparison with the full hypergraph degree distribution. The plot shows the degree distributions  $P(k^*; \mathbf{I}_{\text{real}})$  (blue, circles) and  $P(k^* | C^q = 1; \mathbf{I}_{\text{real}})$  (red, squares) for the six canonical real-hypergraphs considered in this paper. The number of nodes with  $C^q = 1$  are 490 (a), 560 (b), 18 (c), 1683 (d), 12 (e), and 288 (f). Panels represent the different hypergraphs, as explained in the caption of Fig. 5.

of the two hyperedge neighbourhood sets  $\partial_i^{\text{out}}(\mathbf{I}^{\rightarrow})$  and  $\partial_i^{\text{in}}(\mathbf{I}^{\leftarrow})$  where

$$\partial_i^{\text{out}}(\mathbf{I}^{\rightarrow}) \equiv \{\alpha \in \mathcal{H} | I_{i\alpha}^{\rightarrow} \neq 0\}, \quad (61)$$

and

$$\partial_i^{\text{in}}(\mathbf{I}^{\leftarrow}) \equiv \{\alpha \in \mathcal{H} | I_{i\alpha}^{\leftarrow} \neq 0\}. \quad (62)$$

To each directed hypergraph we can associate a projected, directed graph of order  $N$ , such that there exists a directed edge that points from  $i$  to  $j$  in the projected graph whenever there exists a hyperedge  $\alpha \in \mathcal{H}$  such that  $(i, \alpha) \in \mathcal{E}^{\text{out}}$  and  $(j, \alpha) \in \mathcal{E}^{\text{in}}$ . The adjacency matrix of the projected graph is given by

$$A_{ij}^{\text{proj}}(\mathbf{I}^{\leftrightarrow}) = \Theta \left( \sum_{\alpha=1}^M I_{i\alpha}^{\rightarrow} I_{j\alpha}^{\leftarrow} \right), \quad (63)$$

for all  $i, j \in \mathcal{V}$ , where  $\Theta(x) = 0$  if  $x \leq 0$  and  $\Theta(x) = 1$  for  $x > 0$ . If  $A_{ii}^{\text{proj}} = 0$  for all  $i \in \mathcal{V}$ , then we call the projected graph simple.

Note that there exists a one-to-one correspondence between simple, directed hypergraphs  $\mathcal{H}^{\text{dir}}$  and pairs  $\mathbf{I}^{\leftrightarrow}$  of incidence matrices, while the mapping between  $\mathcal{H}$  and  $\mathbf{A}^{\text{proj}}$  is not one-to-one, and hence the projected graph is a coarse-grained representation of the hypergraph.

## B. Clustering coefficient for directed graphs with pairwise interactions

We review the definition of the pairwise clustering coefficient for directed graphs, as introduced in Ref.<sup>26</sup>.

Let  $\mathbf{A}$  be the adjacency matrix of a simple, directed graph, such that  $[\mathbf{A}]_{ij} = 1$  whenever there exists a directed link that points from  $i$  to  $j$ , and  $[\mathbf{A}]_{ij} = 0$  whenever such a link is absent. The directed clustering coefficient of node  $i$  is defined by<sup>26</sup>

$$C_i^{\text{pi}\leftrightarrow}(\mathbf{A}) \equiv \frac{T_i^{\leftrightarrow}(\mathbf{A})}{t_{\max}^{\leftrightarrow}(k_i^{\text{tot}}(\mathbf{A}), k_i^{\leftrightarrow}(\mathbf{A}))}, \quad (64)$$

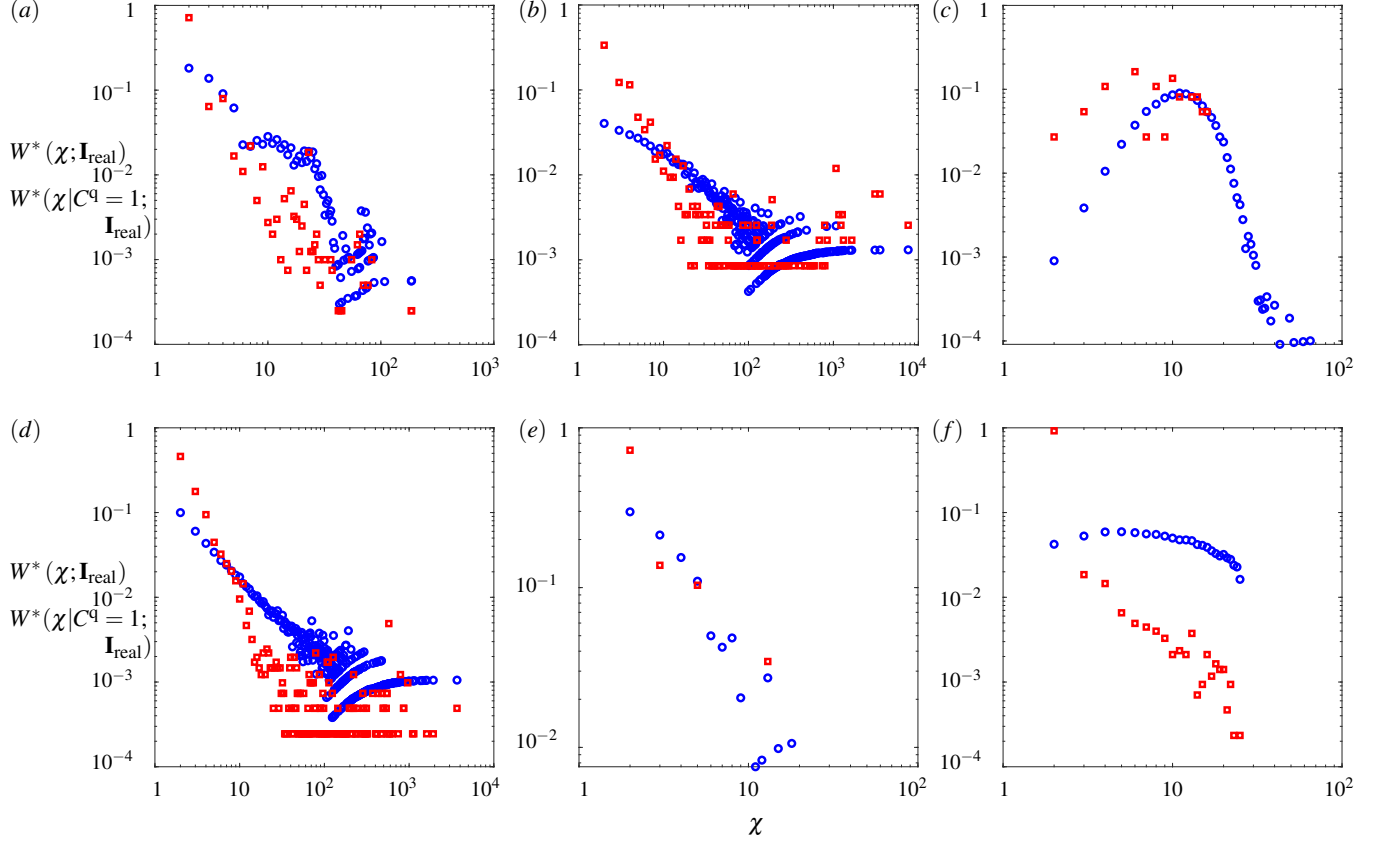


FIG. 10: Distributions of the cardinalities of hyperedges that are incident to a highly clustered node, and comparison with the corresponding distribution for generic nodes. Comparison between the distributions  $W^*(\chi; \mathbf{I}_{\text{real}})$  (blue circles) and  $W^*(\chi | C^q = 1; \mathbf{I}_{\text{real}})$  (red squares) as defined in Eqs. (50) and (51), respectively, for the six canonical real-world hypergraphs considered in this Paper. Panels represent different real-world hypergraphs, as explained in the caption of Fig. 5.

where

$$\begin{aligned} T_i^{\leftrightarrow}(\mathbf{A}) &\equiv \frac{1}{2} [(\mathbf{A} + \mathbf{A}^T)^3]_{ii} \\ &= \frac{1}{2} \sum_{j=1}^N \sum_{h=1}^N (A_{ij} + A_{ji})(A_{ih} + A_{hi})(A_{jh} + A_{hj}) \end{aligned} \quad (65)$$

counts the number of directed triangles centered on node  $i$ , and where

$$t_{\max}^{\leftrightarrow}(k_i^{\text{tot}}(\mathbf{A}), k_i^{\leftrightarrow}(\mathbf{A})) \equiv k_i^{\text{tot}}(\mathbf{A})(k_i^{\text{tot}}(\mathbf{A}) - 1) - k_i^{\leftrightarrow}(\mathbf{A}) \quad (66)$$

is the maximum possible number of directed triangles incident to a node with a given total degree  $k_i^{\text{tot}}(\mathbf{A}) \equiv \sum_{j=1; j \neq i}^N (A_{ij} + A_{ji})$ , and a given degree of symmetric links  $k_i^{\leftrightarrow}(\mathbf{A}) \equiv \sum_{j=1; j \neq i}^N A_{ji}A_{ij}$ . The denominator in the definition of the pairwise clustering coefficient is independent of the directionality and the symmetry (i.e., whether it is unidirectional or bidirection) of the links between node  $i$  and its neighbours. Additionally, for simple and nondirected graphs ( $A_{ij} = A_{ji}$ ) the clustering coefficients in Eqs. (11) and (64) are equal.

Following the example of pairwise clustering coefficients, we define in the next Subsection a quad clustering coefficient

for directed hypergraphs, which is an extension of the corresponding clustering coefficient for nondirected hypergraphs.

### C. Quad clustering coefficient for directed hypergraphs

We define a quad clustering coefficient for directed hypergraphs. Similarly to the pairwise clustering coefficient for directed graphs  $C_i^{\text{pi}\leftrightarrow}$ , we require that the quad clustering coefficient counts the number of directed quads incident to the node  $i$  of a hypergraph, and we require that for nondirected hypergraphs the directed quad clustering coefficient equals the quad clustering coefficient defined in Eq. (13).

We define the quad clustering coefficient  $C_i^{\text{q}\leftrightarrow}(\mathbf{I}^{\leftrightarrow})$  of a node  $i$  in the directed hypergraph represented by  $\mathbf{I}^{\leftrightarrow}$ , for which  $\sum_{\alpha \in \partial_i(\mathbf{I}^{\leftrightarrow})} (\chi_{\alpha,i}^{\text{in}} + \chi_{\alpha,i}^{\text{out}}) \geq 2$ , as follows,

$$C_i^{\text{q}\leftrightarrow}(\mathbf{I}^{\leftrightarrow}) \equiv \frac{Q_i^{\text{q}\leftrightarrow}(\mathbf{I}^{\leftrightarrow})}{q_{\max}^{\text{q}\leftrightarrow}(\{\mathcal{X}_{i\alpha}(\mathbf{I}^{\leftrightarrow}), I_{i\alpha}^{\text{q}\leftrightarrow}\}_{\alpha \in \partial_i})}, \quad (67)$$

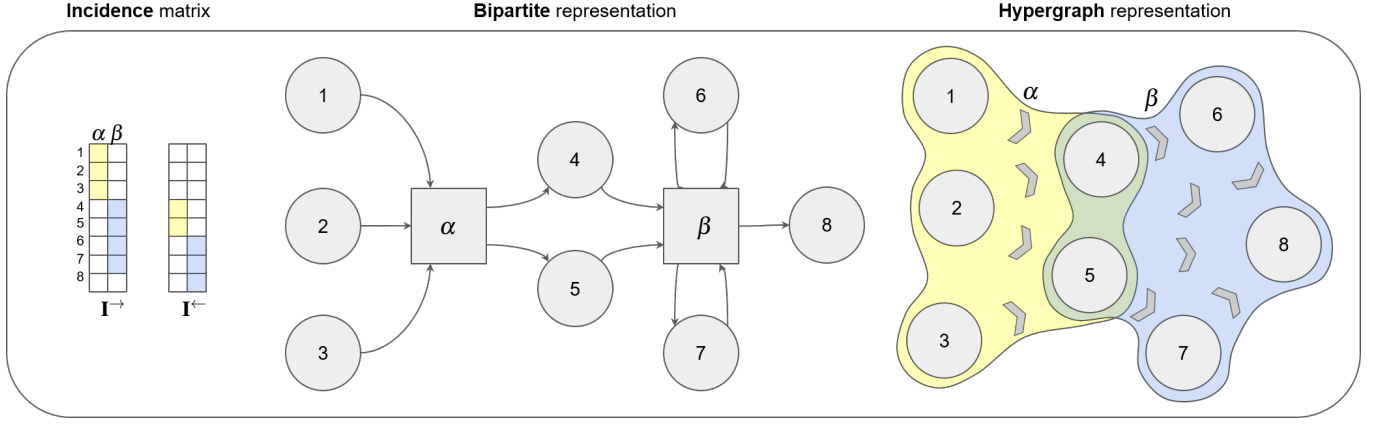


FIG. 11: *Representations of directed hypergraphs.* The figure illustrates with an example the three hypergraph representations, viz., with incidence matrices, as a bipartite graph, or as a graph with higher-order interactions.

where

$$Q_i^{\leftrightarrow}(\mathbf{I}^{\leftrightarrow}) \equiv \sum_{j=1: j \neq i}^N \sum_{\alpha < \beta}^M I_{i\alpha}^{\leftrightarrow} I_{j\alpha}^{\leftrightarrow} I_{i\beta}^{\leftrightarrow} I_{j\beta}^{\leftrightarrow}, \quad (68)$$

is the number of directed quads centred on the node  $i$ , and we have used the notation  $I_{i\alpha}^{\leftrightarrow} \equiv I_{i\alpha}^{\rightarrow} + I_{i\alpha}^{\leftarrow}$ . The denominator  $q_{\max}^{\leftrightarrow}(\{\mathcal{X}_{i\alpha}(\mathbf{I}^{\leftrightarrow}), I_{i\alpha}^{\leftrightarrow}\}_{\alpha \in \partial_i})$  denotes the maximum possible number of directed quads incident to node  $i$ , given the sets

$$\mathcal{X}_{i\alpha}(\mathbf{I}^{\leftrightarrow}) \equiv \left\{ \chi_{\alpha,i}^{\text{in}}(\mathbf{I}^{\rightarrow}), \chi_{\alpha,i}^{\text{out}}(\mathbf{I}^{\leftarrow}) \right\} \quad (69)$$

of modified *in-* and *out-* cardinalities of the hyperedges  $\alpha \in \partial_i$ , and the corresponding values of  $I_{i\alpha}^{\leftrightarrow}$ . We omit the explicit mathematical expression for  $q_{\max}^{\leftrightarrow}$  here, as it is elaborate, but it can be found in Appendix H. If  $\sum_{\alpha \in \partial_i(\mathbf{I}^{\leftrightarrow})} (\chi_{\alpha,i}^{\text{in}} + \chi_{\alpha,i}^{\text{out}}) < 2$  then  $C_i^{\leftrightarrow}(\mathbf{I}) = 0$ . To illustrate how quads are counted by  $Q_i^{\leftrightarrow}(\mathbf{I}^{\leftrightarrow})$ , consider the example in Panel (b) of Fig. 12. In this case,  $Q_i^{\leftrightarrow}(\mathbf{I}^{\leftrightarrow}) = 4$ , as the motif contains the four quads in the left column of Panel (a) of Fig 12.

Alternatively, we can express  $Q_i^{\leftrightarrow}(\mathbf{I}^{\leftrightarrow})$  in terms of the number of closed paths of length 4 (see Panel (a) of Fig 12 for all possible types of closed paths of length 4) with the formula

$$Q_i^{\leftrightarrow}(\mathbf{I}^{\leftrightarrow}) = \frac{1}{2} \left[ (\mathbf{I}^{\leftrightarrow} (\mathbf{I}^{\leftrightarrow})^T)^2 \right]_{ii} - \frac{1}{2} (\mathbf{I}^{\leftrightarrow} (\mathbf{I}^{\leftrightarrow})^T)_{ii}^2 - \frac{1}{2} \sum_{j: j \neq i} \left( (\mathbf{I}^{\leftrightarrow} (\mathbf{I}^{\leftrightarrow})^T)_{ij} \right)^2. \quad (70)$$

The first term  $\left[ (\mathbf{I}^{\leftrightarrow} (\mathbf{I}^{\leftrightarrow})^T)^2 \right]_{ii}$  counts the total number of paths of length 4 starting and ending in  $i$ . The second and third terms subtract off the contributions to the first term arising from paths returning to site  $i$  via backtracking paths of length one and two, respectively. The prefactor 1/2 corrects for double counting arising from counting the same path with the opposite orientation.

Next we turn to the denominator of the right-hand side of (67). Similarly to the pairwise, directed, clustering coefficient  $C_i^{\text{pi}\leftrightarrow}(\mathbf{A})$ , the denominator  $q_{\max}^{\leftrightarrow}(\{\mathcal{X}_{i\alpha}(\mathbf{I}^{\leftrightarrow}), I_{i\alpha}^{\leftrightarrow}\}_{\alpha \in \partial_i})$

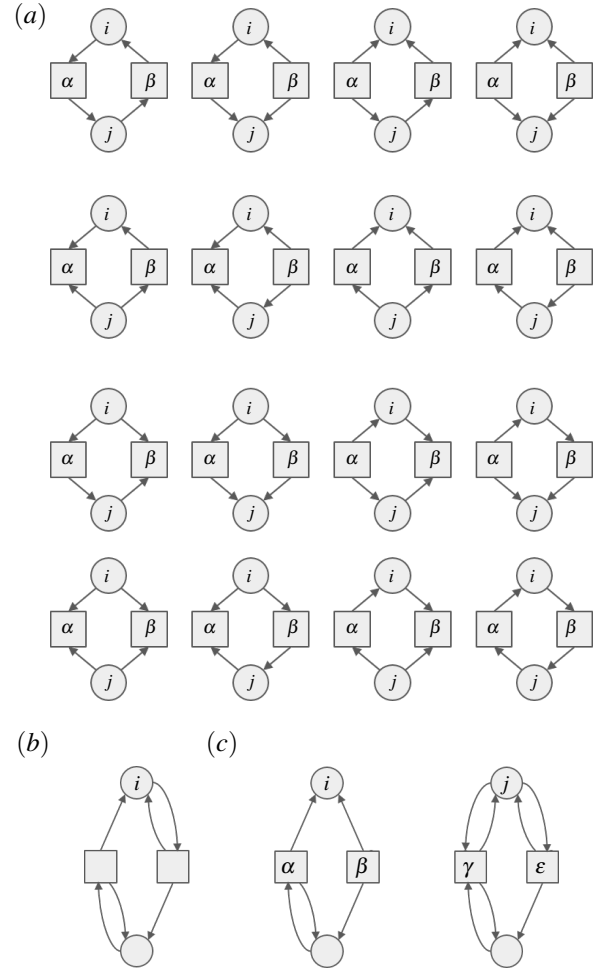


FIG. 12: *Counting the number of directed quads incident to a node  $i$ .* (a) The 16 directed quads that contribute to  $Q_i^{\text{q}}(\mathbf{I})$ . (b) Example graph with  $C_i^{\text{q},\leftrightarrow} = 1$ . (c) Two example graphs with  $C_i^{\text{q},\leftrightarrow} = C_j^{\text{q},\leftrightarrow} = 1$ .

normalizes the directed quad clustering coefficient  $C_i^{q\leftrightarrow}(\mathbf{I}^{\leftrightarrow})$  such that its value is independent of both the directionality and symmetry (i.e., unidirectional or bidirectional) of the links that connect node  $i$  to its neighbouring hyperedges. This means that if two nodes  $i$  and  $j$  have the same motif of inlinks, as shown in Panel (c) of Fig 12, then the quad clustering coefficient of the two nodes,  $C_i^{q\leftrightarrow}$  and  $C_j^{q\leftrightarrow}$ , must be the same, even if the motifs of outlinks are different.

Note that for nondirected hypergraphs the directed quad clustering coefficient, defined by Eq. (67), equals the quad clustering coefficient for nondirected hypergraphs, defined by Eq. (13) (see Appendix I).

#### D. Clustering in directed, realworld, hypergraphs

In Sec. V we found that the density of quads in nondirected real-world hypergraphs is large compared to the density of quads in the configuration model. In this Section, we investigate whether an analogous phenomenon can be observed in directed hypergraphs. Specifically, we build directed hypergraphs from three data sets related to the DNC-email network, the English thesaurus, and the Human metabolic pathway (see Appendix F for more detailed information about these data sets).

In Table II we present the mean quad clustering coefficient  $\bar{C}^{q\leftrightarrow}(\mathbf{I}_{\text{real}}) \equiv \frac{1}{N} \sum_{i=1}^N C_i^{q\leftrightarrow}(\mathbf{I}_{\text{real}})$  for the three real-world hypergraphs under study, and compare their values with the corresponding directed configuration models, which have the prescribed degree sequences  $\bar{k}^{\text{in}}(\mathbf{I}_{\text{real}})$  and  $\bar{k}^{\text{out}}(\mathbf{I}_{\text{real}})$ , and the prescribed cardinality sequences  $\bar{\chi}^{\text{in}}(\mathbf{I}_{\text{real}})$  and  $\bar{\chi}^{\text{out}}(\mathbf{I}_{\text{real}})$ . We observe that the real-world networks have significantly larger directed quad clustering coefficient, up to 500 times larger than those of corresponding random models. Hence, the density of directed quads in real-world directed hypergraphs is significantly higher than their density in the corresponding configuration models, consistent with earlier findings for nondirected hypergraphs.

Furthermore, we determine the distribution of directed, quad clustering coefficients in real-world hypergraphs defined by  $P(C^{q\leftrightarrow}; \mathbf{I}_{\text{real}}) \equiv \frac{1}{N} \sum_{i=1}^N \delta(C^{q\leftrightarrow} - C_i^{q\leftrightarrow}(\mathbf{I}_{\text{real}}))$ , and present the results in Fig. 13. Also in directed real-world hypergraphs, we observe a peak at  $C^{q\leftrightarrow} \approx 1$  in the quad clustering distribution. In the specific examples considered, the peak is most pronounced in the DNC-email hypergraph.

TABLE II: Network characteristics of the real-world directed hypergraphs: number of nodes  $N$  and hyperedges  $M$ , mean directed quad clustering coefficient  $\bar{C}^{q\leftrightarrow}(\mathbf{I}_{\text{real}})$  and the average, mean directed quad clustering coefficient  $\langle \bar{C}^{q\leftrightarrow}(\mathbf{I}^{\leftrightarrow}) \rangle$  of the corresponding configuration model.

| Dataset            | $N$    | $M$    | $\bar{C}^{q\leftrightarrow}(\mathbf{I}_{\text{real}})$ | $\langle \bar{C}^{q\leftrightarrow}(\mathbf{I}^{\leftrightarrow}) \rangle$ |
|--------------------|--------|--------|--|--|
| DNC-email          | 2,029  | 5,598  | 0.3419   | 0.0715   |
| English thesaurus  | 40,963 | 35,104 | 0.2371   | 0.0004   |
| Metabolic pathways | 1,508  | 1,451  | 0.0684   | 0.0179   |

## VII. DISCUSSION

We have introduced a clustering coefficient, called the quad clustering coefficient, that captures the multiplicity of interactions between neighbouring nodes in (non)directed hypergraphs with higher order interactions. We have shown that for random hypergraphs the mean quad clustering coefficient has a value near zero, while for real-world networks it is one order of magnitude larger taking values ranging from 0.01 to 0.34, which is a smaller range than the one observed for pairwise clustering coefficients in real-world networks<sup>27</sup>; we note however that the distribution of quad clustering coefficients is supported on the whole  $[0, 1]$  range of values. Hence, the quad clustering coefficient describes a feature of real-world networks that is not captured by the current random hypergraph models.

We have determined the average quad clustering coefficient in several random hypergraph models. We have obtained exact expressions for models with fluctuating degrees and fixed cardinalities. Our analysis shows that it is significantly more difficult to deal with fluctuating cardinalities.

Analysing the distribution of quad clustering coefficients in real-world networks we have found that there exist a significant fraction of nodes that take its maximal value. Analysing the topological properties of the neighbourhood sets of these highly clustered nodes we have found that they can exhibit large degrees, and their neighbouring nodes can have large cardinalities.

The results of this paper show that the configuration model is not a good null model for real-world networks with higher order interactions. This in itself is not a surprising result, as the configuration model is also not a good model for networks without higher order interactions, see e.g., discussions in Ref.<sup>6</sup>. However, what is surprising is that the distribution of quad clustering coefficients exhibits a peak at its maximal value. This result has, to the best of our knowledge, no counterpart in systems without higher order interactions.

This raises the question of what type of random hypergraph model can generate statistical properties similar to those observed in real-world networks with higher order interactions, see e.g., Ref.<sup>5,7,8</sup> for related questions in networks without higher order interactions. Another pertinent question concerns the implications of nodes with high quad clustering coefficients on dynamical processes, such as, percolation. Since highly clustered nodes do not appear in random hypergraphs, they may play an important role in dynamical processes governed on real-world networks.

## ACKNOWLEDGMENTS

G.-G. Ha thanks D.-S. Lee, J.W. Lee, S.H. Lee, S.-W. Son, H.J. Park, M. Ha and N.W. Landry. This work was supported by the Engineering and Physical Sciences Research Council, part of the EPSRC DTP, Grant Ref No.: EP/V520019/1.



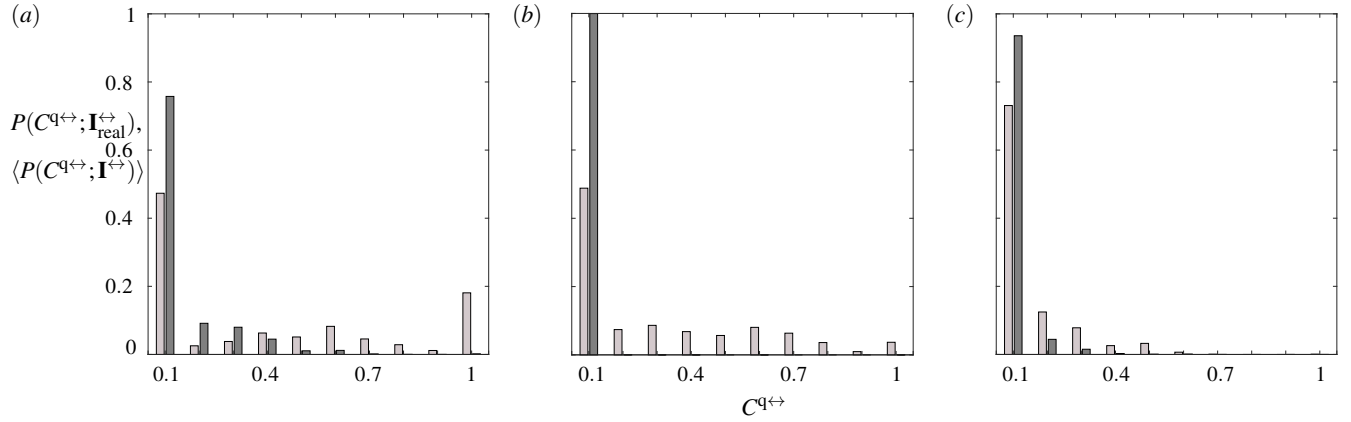


FIG. 13: *Distribution of quad clustering coefficients in directed hypergraphs.* The light grey histograms represent the distributions of the directed quad clustering coefficient measured in real-world hypergraphs. The grey bar graphs show the distributions of the directed quad clustering coefficient measured in the hypergraph configuration model that preserves the in-/out-degree and in-/out-cardinality sequences extracted from the real-world hypergraphs. Each plots are extracted from (a) *DNC-email*, (b) *English thesaurus*, (c) *Human metabolic pathways*

#### DATA AVAILABILITY STATEMENT

We used the databases *NDC-substances*<sup>28</sup>, *Youtube*<sup>29,30</sup>, *Food recipe*<sup>31</sup>, *Github*<sup>29,32</sup>, *Crime involvement*<sup>29</sup> and *Walmart*<sup>33</sup> as the real-world undirected hypergraph. And as a directed hypergraph, we used *DNC-email*<sup>29</sup>,

*English thesaurus*<sup>34</sup> and *Human metabolic pathways*<sup>35</sup> database. And we implemented computation algorithms in Fortran to compute nondirected and directed quad clustering coefficients in a hypergraph, available from <https://github.com/Gyeong-GyunHa/qch>.

#### Appendix A: Alternate expression for the denominator of the quad clustering coefficient

In this Section we show that  $q_{\max}$ , defined by Eq. (16), can also be expressed by Eq. (17).

We can express Eq. (16)

$$2q_{\max} = \sum_{\substack{\alpha, \beta; \\ \chi_{\alpha}(\mathbf{I}) \leq \chi_{\beta}(\mathbf{I})}} \chi_{\alpha}(\mathbf{I}) I_{i\alpha} I_{i\beta} - \sum_{\substack{\alpha, \beta; \\ \chi_{\alpha}(\mathbf{I}) = \chi_{\beta}(\mathbf{I})}} \chi_{\alpha}(\mathbf{I}) I_{i\alpha} I_{i\beta} + \sum_{\substack{\alpha, \beta; \\ \chi_{\alpha}(\mathbf{I}) \geq \chi_{\beta}(\mathbf{I})}} \chi_{\beta}(\mathbf{I}) I_{i\alpha} I_{i\beta} - \sum_{\alpha, \beta} I_{i\alpha} I_{i\beta} - \sum_{\alpha} (\chi_{\alpha}(\mathbf{I}) - 1) I_{i\alpha}. \quad (\text{A1})$$

To proceed, we introduce the definitions

$$\Omega_i(\mathbf{I}) \equiv \sum_{\gamma=1}^M I_{i\gamma} \chi_{\gamma}(\mathbf{I}) \quad (\text{A2})$$

and

$$q_{i, \chi}(\vec{\chi}(\mathbf{I}); \mathbf{I}) \equiv \sum_{\alpha: \chi_{\alpha}(\mathbf{I})} I_{i\alpha} = \sum_{\alpha} I_{i\alpha} \Theta(\chi_{\alpha}(\mathbf{I}) - \chi), \quad (\text{A3})$$

where  $\Theta(\chi_\alpha(\mathbf{I}) - \chi)$  is the Heaviside function defined below Eq. (10). Using these definitions in Eq. (A1), yields

$$2q_{\max} = \sum_{\alpha=1}^M \chi_\alpha(\mathbf{I}) I_{i\alpha} q_{i,\chi_\alpha(\mathbf{I})}(\vec{\chi}(\mathbf{I}); \mathbf{I}) - \sum_{\substack{\alpha,\beta=1; \\ \chi_\alpha(\mathbf{I})=\chi_\beta(\mathbf{I})}}^M \chi_\alpha(\mathbf{I}) I_{i\alpha} I_{i\beta} + \sum_{\substack{\alpha,\beta=1; \\ \chi_\alpha(\mathbf{I})\geq\chi_\beta(\mathbf{I})}}^M \chi_\beta(\mathbf{I}) I_{i\alpha} I_{i\beta} - k_i^2(\mathbf{I}) - \Omega_i(\mathbf{I}) + k_i(\mathbf{I}) \quad (\text{A4})$$

$$= 2 \sum_{\alpha=1}^M \chi_\alpha(\mathbf{I}) I_{i\alpha} q_{i,\chi_\alpha(\mathbf{I})}(\vec{\chi}(\mathbf{I}); \mathbf{I}) - \sum_{\alpha=1}^M \chi_\alpha(\mathbf{I}) I_{i\alpha} \left[ q_{i,\chi_\alpha(\mathbf{I})}(\vec{\chi}(\mathbf{I}); \mathbf{I}) - q_{i,\chi_\alpha(\mathbf{I})}(\vec{\chi}(\mathbf{I}) - \vec{1}; \mathbf{I}) \right] - k_i^2(\mathbf{I}) - \Omega_i(\mathbf{I}) + k_i(\mathbf{I}) \quad (\text{A5})$$

$$= \sum_{\alpha=1}^M \chi_\alpha(\mathbf{I}) I_{i\alpha} \left[ q_{i,\chi_\alpha(\mathbf{I})}(\vec{\chi}(\mathbf{I}); \mathbf{I}) + q_{i,\chi_\alpha(\mathbf{I})}(\vec{\chi}(\mathbf{I}) - \vec{1}; \mathbf{I}) \right] - k_i^2(\mathbf{I}) - \Omega_i(\mathbf{I}) + k_i(\mathbf{I}) \quad (\text{A6})$$

$$= \sum_{\alpha=1}^M \chi_\alpha(\mathbf{I}) I_{i\alpha} \left[ q_{i,\chi_\alpha(\mathbf{I})}(\vec{\chi}(\mathbf{I}); \mathbf{I}) + q_{i,\chi_\alpha(\mathbf{I})}(\vec{\chi}(\mathbf{I}) - \vec{1}; \mathbf{I}) - 1 \right] + k_i(\mathbf{I}) - k_i^2(\mathbf{I}) \quad (\text{A7})$$

$$= \sum_{\chi=1}^N \chi \sum_{\alpha} \delta_{\chi,\chi_\alpha(\mathbf{I})} I_{i\alpha} \left[ q_{i,\chi_\alpha(\mathbf{I})}(\vec{\chi}(\mathbf{I}); \mathbf{I}) + q_{i,\chi_\alpha(\mathbf{I})}(\vec{\chi}(\mathbf{I}) - \vec{1}; \mathbf{I}) - 1 \right] + k_i(\mathbf{I}) - k_i^2(\mathbf{I}) \quad (\text{A8})$$

$$= \sum_{\chi=1}^N \chi \left( \sum_{\alpha} \delta_{\chi,\chi_\alpha(\mathbf{I})} I_{i\alpha} \right) \left[ q_{i,\chi}(\vec{\chi}(\mathbf{I}); \mathbf{I}) + q_{i,\chi}(\vec{\chi}(\mathbf{I}) - \vec{1}; \mathbf{I}) - 1 \right] + k_i(\mathbf{I}) - k_i^2(\mathbf{I}) \quad (\text{A9})$$

$$= \sum_{\chi=1}^N \chi \left[ q_{i,\chi}(\vec{\chi}(\mathbf{I}); \mathbf{I}) - q_{i,\chi}(\vec{\chi}(\mathbf{I}) - \vec{1}; \mathbf{I}) \right] \left[ q_{i,\chi}(\vec{\chi}(\mathbf{I}); \mathbf{I}) + q_{i,\chi}(\vec{\chi}(\mathbf{I}) - \vec{1}; \mathbf{I}) - 1 \right] + k_i(\mathbf{I}) - k_i^2(\mathbf{I}) \quad (\text{A10})$$

$$= \sum_{\chi=1}^N \chi \left[ (q_{i,\chi}(\vec{\chi}(\mathbf{I}); \mathbf{I}))^2 - (q_{i,\chi}(\vec{\chi}(\mathbf{I}) - \vec{1}; \mathbf{I}))^2 - q_{i,\chi}(\vec{\chi}(\mathbf{I}); \mathbf{I}) + q_{i,\chi}(\vec{\chi}(\mathbf{I}) - \vec{1}; \mathbf{I}) \right] + q_{i,1}(\vec{\chi}(\mathbf{I}); \mathbf{I}) - (q_{i,1}(\vec{\chi}(\mathbf{I}); \mathbf{I}))^2 \quad (\text{A11})$$

$$= \sum_{\chi=2}^N q_{i,\chi}(\vec{\chi}(\mathbf{I}); \mathbf{I}) [q_{i,\chi}(\vec{\chi}(\mathbf{I}); \mathbf{I}) - 1], \quad (\text{A12})$$

where  $\vec{1}$  is the vector of  $M$  entries, all equal to one. Note that the passage from (A8) to (A9) we have used

$$\begin{aligned} \sum_{\alpha} \delta_{\chi,\chi_\alpha(\mathbf{I})} I_{i\alpha} [q_{i,\chi_\alpha(\mathbf{I})}(\vec{\chi}(\mathbf{I}); \mathbf{I})] &= \sum_{\alpha} \delta_{\chi,\chi_\alpha(\mathbf{I})} I_{i\alpha} \left[ \sum_{\beta \neq \alpha} I_{i\beta} \Theta(\chi_\beta(\mathbf{I}) - \chi_\alpha(\mathbf{I})) \right] \\ &= \sum_{\alpha} \delta_{\chi,\chi_\alpha(\mathbf{I})} I_{i\alpha} \left[ \sum_{\beta \neq \alpha} I_{i\beta} \Theta(\chi_\beta(\mathbf{I}) - \chi) \right] = \sum_{\alpha} \delta_{\chi,\chi_\alpha(\mathbf{I})} I_{i\alpha} \left[ \sum_{\beta} I_{i\beta} \Theta(\chi_\beta(\mathbf{I}) - \chi) \right] \end{aligned} \quad (\text{A13})$$

Using the degrees  $k_i(\mathbf{I}; \chi)$  as defined in Eq. (6), we can express  $q_{i,\chi}$  by

$$q_{i,\chi}(\vec{\chi}(\mathbf{I}); \mathbf{I}) = \sum_{\lambda=\chi}^N k_i(\mathbf{I}; \lambda), \quad (\text{A14})$$

and using this expression in Eq. (A12) we find

$$\begin{aligned} q_{\max}(\{k_i(\chi)\}_{\chi \in \mathbb{N}}) &= \frac{1}{2} \sum_{\chi=2}^N q_{i,\chi}(\vec{\chi}(\mathbf{I}); \mathbf{I}) [q_{i,\chi}(\vec{\chi}(\mathbf{I}); \mathbf{I}) - 1] \\ &= \frac{1}{2} \sum_{\chi=2}^N \left[ \left( \sum_{\lambda=\chi}^{\infty} k_i(\mathbf{I}; \lambda) \right) \left( \sum_{\lambda=\chi}^{\infty} k_i(\mathbf{I}; \lambda) - 1 \right) \right] \\ &= \frac{1}{2} \sum_{\chi=2}^N (\chi - 1) k_i(\chi) \left( \sum_{\chi'=\chi}^{\infty} k_i(\chi') - 1 \right), \end{aligned} \quad (\text{A15})$$

which is the equality (17) in the main text, which we were meant to show.

## Appendix B: Asymptotic expression of Lind's and Zhang's clustering coefficients for large cardinalities

We show that Eqs. (21) and (25) recover Eqs. (18) and (22) if  $i$  is connected to two hyperedges  $\alpha$  and  $\beta$  and if the cardinality  $\chi_\alpha \rightarrow \infty$  with the ratio  $r = \chi_\beta/\chi_\alpha > 1$  fixed.

### 1. Lind's clustering coefficient

If node  $i$  is connected two hyperedges  $\alpha$  and  $\beta$ , Lind's clustering coefficient takes the form

$$C_i^{\text{Lind}} = \frac{Q_i}{(\chi_\alpha - 1 - Q_i)(\chi_\beta - 1 - Q_i) + Q_i}. \quad (\text{B1})$$

For large values of  $\chi_\alpha$ , we can set  $\chi_\beta = r\chi_\alpha$  and  $Q_i = q\chi_\alpha$ , which yields, after neglecting leading order terms, the expression

$$C_i^{\text{Lind}} = \frac{q\chi_\alpha}{\chi_\alpha^2(1-q)(r-q) + \chi_\alpha q} = \frac{q}{\chi_\alpha(1-q)(r-q) + q}. \quad (\text{B2})$$

### 2. Zhang's clustering coefficient

If node  $i$  is only connected to hyperedges  $\alpha$  and  $\beta$ , then Zhang's clustering coefficient takes the form

$$C_i^{\text{Zhang}} = \frac{Q_i}{(\chi_\alpha - 1) + (\chi_\beta - 1) - Q_i}, \quad (\text{B3})$$

For large values of  $\chi_\alpha$ , we can set  $\chi_\beta = r\chi_\alpha$  and  $Q_i = q\chi_\alpha$  as same as previous subsection. After neglecting leading order terms, the expression

$$C_i^{\text{Zhang}} = \frac{Q_i}{(\chi_\alpha - 1)(1+r) - Q_i} = \frac{q}{1+r-q}. \quad (\text{B4})$$

## Appendix C: Explanation of the two configurations for $C_i^{\text{Lind}}$ considered in the lower panel of Fig. 3

In the lower panel of Fig. 3 we consider motifs consisting of a central node  $i$ , three hyperedges  $\alpha$ ,  $\beta$ , and  $\gamma$ , and a given number  $Q_i(\mathbf{I})$  of quads. There are different ways of assigning quads to a given node  $i$  and three hyperedges, and this leads to different values of the Lind clustering coefficients  $C_i^{\text{Lind}}$ , as shown in Fig. 3. In this Appendix, we specify the two ways of assigning quads to  $i$  that have been considered in Fig. 3 and which we call the uniform and the biased case. Since there are three hyperedges, the different ways of assigning quads to these three hyperedges are fully determined by the numbers  $q_{i\alpha\beta}(\mathbf{I})$ ,  $q_{i\beta\gamma}(\mathbf{I})$ , and  $q_{i\alpha\gamma}(\mathbf{I})$  that denote the number of quads incident to node  $i$  and two given hyperedges (see Eq. (15) for the definition). The example considered in Fig. 3 has cardinalities  $\chi_\alpha = 15$ ,  $\chi_\beta = 20$ , and  $\chi_\gamma = 25$ , and therefore we focus on this case.

### 1. Uniform case

In the uniform case, we assign uniformly and sequentially quads to the three hyperedges  $\alpha$ ,  $\beta$ , and  $\gamma$ . This gives

$$q_{i\alpha\beta}(Q_i(\mathbf{I})) = \sum_{a=0}^{13} \Theta(Q_i(\mathbf{I}) - 3a), \quad q_{i\alpha\gamma}(Q_i(\mathbf{I})) = \sum_{a=0}^{13} \Theta(Q_i(\mathbf{I}) - 3a - 2), \quad (\text{C1})$$

and

$$q_{i\beta\gamma}(Q_i(\mathbf{I})) = \sum_{a=0}^{13} \Theta(Q_i(\mathbf{I}) - 3a - 1) + \sum_{b=42}^{46} \Theta(Q_i(\mathbf{I}) - b), \quad (\text{C2})$$

where  $\Theta(x)$  is the Heaviside function as defined below Eq. (10). We illustrate this configuration in Panel (a) of Fig. 14 for the case of  $Q_i(\mathbf{I}) = 6$ .

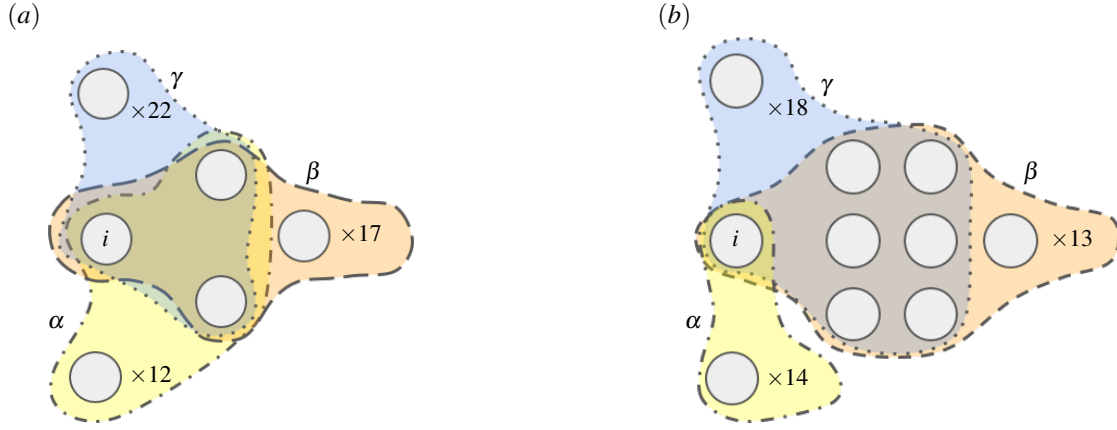


FIG. 14: Illustration of the configurations of quads in the uniform and biased case as defined in Appendices C 1 and C 2, respectively, for the case  $Q_i = 6$ . The yellow shaded area bounded by a dash-dotted line denotes hyperedge  $\alpha$ ; the blue shaded area bounded by a dashed line represents hyperedge  $\beta$ ; and the orange shaded area with a dotted border represents hyperedge  $\gamma$ . Panel (a): Three nodes, viz.,  $i$  and two other nodes, are incident to the three hyperedges  $\alpha$ ,  $\beta$ , and  $\gamma$ , yielding  $Q_i = 6$ . Panel (b): Seven nodes, viz.,  $i$  and six other nodes, are incident to the two hyperedges  $\gamma$  and  $\beta$ , yielding  $Q_i = 6$ .

## 2. Biased case

This is the opposing case where quads are fully assigned to one hyperedge, before assigning them to the other hyperedges. In this case, we get

$$q_{i\alpha\beta}(Q_i(\mathbf{I})) = \sum_{a=24}^{28} \Theta(Q_i(\mathbf{I}) - a) + \sum_{b=34}^{38} \Theta(Q_i(\mathbf{I}) - b) + \sum_{c=43}^{46} \Theta(Q_i(\mathbf{I}) - c), \quad (\text{C3})$$

$$q_{i\alpha\gamma}(Q_i(\mathbf{I})) = \sum_{a=19}^{23} \Theta(Q_i(\mathbf{I}) - a) + \sum_{b=29}^{33} \Theta(Q_i(\mathbf{I}) - b) + \sum_{c=39}^{42} \Theta(Q_i(\mathbf{I}) - c),$$

and

$$q_{i\beta\gamma}(Q_i(\mathbf{I})) = \sum_{a=0}^{18} \Theta(Q_i(\mathbf{I}) - a). \quad (\text{C4})$$

In Panel (b) of Fig. 14 we illustrate the biased case when  $Q_i(\mathbf{I}) = 6$ .

## Appendix D: Average quad clustering coefficient for random hypergraph models with regular cardinalities

Building on random graph methods as developed in Refs. <sup>1-3,25</sup>, we derive in this Appendix the expressions (31), (34) and (36) for the average quad clustering coefficients of random hypergraph models with regular cardinalities. In Appendix D 1, we derive Eq. (31), and in Appendix D 2, we derive Eq. (36). Since (34) is a special limiting case of (36), we do not discuss it separately.

### 1. $\chi$ -regular ensemble

We derive the formula (31) for the average quad clustering coefficient of hypergraphs drawn from the ensemble  $P_\chi(\mathbf{I})$  as defined in Eq. (27).

#### a. Normalisation constant of $P_\chi$

The normalisation constant in Eq. (27) is given by

$$\mathcal{N}_\chi = \sum_{\mathbf{I}} \prod_{\gamma=1}^M \delta_{\chi, \chi_\gamma(\mathbf{I})} = \left[ \binom{N}{\chi} \right]^M, \quad (\text{D1})$$

as each hyperedge is connected to  $\chi$  nodes that are randomly selected from the  $N$  available options.

### b. Average clustering coefficient

Substituting the definition of the quad clustering coefficient, Eq. (13), into the expression (28) for the ensemble average clustering coefficient yields

$$\begin{aligned}
\mathcal{N}_\chi \langle C_i^q(\mathbf{I}) \rangle_\chi &= \frac{1}{\chi-1} \left\langle \sum_{q=2}^{\infty} \delta_{q,k_i(\mathbf{I})} \delta_{\chi\bar{1},\bar{\chi}(\mathbf{I})} \frac{\sum_{\alpha,\beta,\alpha<\beta} \sum_{g \notin \{i\}} I_{g\alpha} I_{g\beta} I_{i\alpha} I_{i\beta}}{\sum_{\alpha<\beta} I_{i\alpha} I_{i\beta}} \right\rangle \\
&= \sum_{q=2}^{\infty} \frac{2}{q(q-1)(\chi-1)} \sum_{\alpha,\beta,\alpha<\beta} \sum_{j=1;j \neq i}^N \left\langle \delta_{q,k_i(\mathbf{I})} \delta_{\chi\bar{1},\bar{\chi}(\mathbf{I})} I_{j\alpha} I_{j\beta} I_{i\alpha} I_{i\beta} \right\rangle_\chi \\
&= \sum_{q=2}^{\infty} \frac{2}{q(q-1)(\chi-1)} \int_0^{2\pi} \frac{d\hat{q}}{2\pi} e^{i\hat{q}q} \int_{[0,2\pi]^M} \prod_{\xi=1}^M \frac{d\hat{\xi}}{2\pi} e^{i\hat{\xi}\xi} \\
&\times \sum_{\alpha,\beta,\alpha<\beta} \sum_{j=1;j \neq i}^N \left\langle e^{-i\hat{q}k_i(\mathbf{I})} \prod_{\xi'=1}^M e^{-i\hat{\xi}' \sum_{\sigma} I_{\sigma\xi'}} I_{j\alpha} I_{j\beta} I_{i\alpha} I_{i\beta} \right\rangle, \tag{D2}
\end{aligned}$$

where we have used the notation

$$\langle f(\mathbf{I}) \rangle \equiv \sum_{\mathbf{I} \in \{0,1\}^{NM}} f(\mathbf{I}). \tag{D3}$$

Performing the sum over all the entries  $I_{j\alpha}$  of the incidence matrix  $\mathbf{I}$  yields

$$\begin{aligned}
\mathcal{N}_\chi \langle C_i^q(\mathbf{I}) \rangle_\chi &= \sum_{q=2}^{\infty} \frac{2}{q(q-1)(\chi-1)} \int_0^{2\pi} \frac{d\hat{q}}{2\pi} e^{i\hat{q}q} \int_{[0,2\pi]^M} \prod_{\xi=1}^M \frac{d\hat{\xi}}{2\pi} e^{i\hat{\xi}\xi} \\
&\times \sum_{\alpha,\beta,\alpha<\beta} \sum_{j=1;j \neq i}^N e^{-2i\hat{q}} e^{-2i\hat{\xi}\alpha} e^{-2i\hat{\xi}\beta} \prod_{\gamma \notin \{\alpha,\beta\}} \left[ e^{-i\hat{q}} e^{-i\hat{\xi}\gamma} + 1 \right] \\
&\times \left( e^{-i\hat{\xi}\epsilon} + 1 \right)^{N-1} \left( e^{-i\hat{\xi}\alpha} + 1 \right)^{N-2} \left( e^{-i\hat{\xi}\beta} + 1 \right)^{N-2}. \tag{D4}
\end{aligned}$$

Expanding the power expressions in (D4) and integrating over the  $\hat{\xi}_\gamma$  variables we get

$$\mathcal{N}_\chi \langle C_i^q(\mathbf{I}) \rangle = \sum_{q=2}^{\infty} \frac{M(M-1)(N-1)}{q(q-1)(\chi-1)} \int_0^{2\pi} \frac{d\hat{q}}{2\pi} e^{i\hat{q}q} e^{-2i\hat{q}} \left( \frac{N-2}{\chi-2} \right)^2 \left( \left( \frac{N-1}{\chi-1} \right) e^{-i\hat{q}} + \left( \frac{N-1}{\chi} \right) \right)^{M-2}. \tag{D5}$$

Further, expanding the power in (D5) and integrating over  $\hat{q}$  reduces the expression into

$$\mathcal{N}_\chi \langle C_i^q(\mathbf{I}) \rangle = \frac{\chi-1}{N-1} \left\{ \left[ \left( \frac{N-1}{\chi-1} \right) + \left( \frac{N-1}{\chi} \right) \right]^M - \left[ \left( \frac{N-1}{\chi} \right) \right]^M - M \left( \frac{N-1}{\chi-1} \right) \left( \frac{N-1}{\chi} \right)^{M-1} \right\}. \tag{D6}$$

Lastly, dividing (D6) by the normalisation constant (D1) gives Eq. (31), which we were meant to derive.

## 2. $\chi$ -regular with prescribed degree sequence

We derive the formula (36) for the average quad clustering coefficient of the  $\chi$ -regular hypergraph ensemble with a prescribed degree sequence  $\vec{k}$ , as defined in Eq. (35), in the limit  $N \rightarrow \infty$  with fixed ratio

$$\mu \equiv \frac{M}{N} = \frac{c}{\chi}, \tag{D7}$$

and where

$$c \equiv \frac{\sum_{j=1}^N k_j}{N}. \tag{D8}$$

The calculations are facilitated by rewriting the expression for  $P_{\vec{k},\chi}$  in the following form

$$P_{\vec{k},\chi}(\mathbf{I}) = \frac{1}{\mathcal{M}_{\vec{k},\chi}} \prod_{i=1}^N \prod_{\alpha=1}^M [p_* \delta_{I_{i\alpha},1} + (1-p_*) \delta_{I_{i\alpha},0}] \prod_{j=1}^N \delta_{k_j,k_j(\mathbf{I})} \prod_{\alpha=1}^M \delta_{\chi,\chi_\alpha(\mathbf{I})} \quad (\text{D9})$$

where  $\mathcal{M}_{\vec{k},\chi}$  is the new normalisation constant that depends on the value of  $p_* \in [0, 1]$ . When  $p_* = 1/2$ , we recover the expression Eq. (35). Introducing a value  $p_* \neq 1/2$  is a calculation trick that does not affect the average value of observables, such as  $\langle C_i^q \rangle_{\vec{k},\chi}$ , but it does alter the normalisation constant.

In Appendix D 2 a, we determine the normalisation constant  $\mathcal{M}_{\vec{k},\chi}$ , and in Appendix D 2 b we calculate the average clustering coefficient.

### a. Normalisation constant of $P_{\vec{k},\chi}$

From the definition of  $\mathcal{M}_{\vec{k},\chi}$  as the normalisation constant of  $P_{\vec{k},\chi}$ , as defined in Eq. (D9), it follows that

$$\begin{aligned} \mathcal{M}_{\vec{k},\chi} &= \sum_{\mathbf{I}} \prod_{i,\alpha} [p_* \delta_{I_{i\alpha},1} + (1-p_*) \delta_{I_{i\alpha},0}] \prod_{j=1}^N \delta_{k_j,k_j(\mathbf{I})} \prod_{\gamma=1}^M \delta_{\chi,\chi_\gamma(\mathbf{I})} \\ &= \sum_{\mathbf{I}} \int_{[0,2\pi]^N} \prod_{j=1}^N \frac{d\hat{k}_j}{2\pi} e^{i\hat{k}_j k_j} \int_{[0,2\pi]^M} \prod_{\gamma=1}^M \frac{d\hat{\Xi}_\gamma}{2\pi} e^{i\hat{\Xi}_\gamma \chi} \prod_{i,\alpha} [p_* \delta_{I_{i\alpha},1} e^{-i\hat{k}_i} e^{-i\hat{\Xi}_\alpha} + (1-p_*) \delta_{I_{i\alpha},0}], \end{aligned} \quad (\text{D10})$$

where we have expressed the Kronecker delta functions as integrals in order to get an expression that factorises in the  $\mathbf{I}$  variables.

Summing over the  $\mathbf{I}$ -variables we get

$$\mathcal{M}_{\vec{k},\chi} = \int \prod_{j=1}^N \frac{d\hat{k}_j}{2\pi} e^{i\hat{k}_j k_j} \int \prod_{\gamma=1}^M \frac{d\hat{\Xi}_\gamma}{2\pi} e^{i\hat{\Xi}_\gamma \chi} \prod_{i,\alpha} [p_* e^{-i\hat{k}_i - i\hat{\Xi}_\alpha} + 1 - p_*]. \quad (\text{D11})$$

We set  $p_* = \rho_*/N$  and take the limit  $N \rightarrow \infty$  for fixed  $M/N$  to obtain

$$\prod_{\alpha=1}^M \left[ 1 + \frac{\rho_*}{N} \left( e^{-i\hat{k}_i - i\hat{\Xi}_\alpha} - 1 \right) \right] = \exp \left[ \rho_* M \frac{e^{-i\hat{k}_i}}{N} \frac{\sum_{\alpha=1}^M e^{-i\hat{\Xi}_\alpha}}{M} - \frac{\rho_* M}{N} + \mathcal{O}(1/N) \right], \quad (\text{D12})$$

where  $\mathcal{O}(1/N)$  represents a subleading order term that decays as  $\sim 1/N$  for large values of  $N$ . The constant  $\rho_* \in \mathbb{R}_+$  is an arbitrary constant that determines the normalisation constant but disappears in the final expression of the average clustering coefficient. Identifying the term  $\sum_{\alpha=1}^M e^{-i\hat{\Xi}_\alpha}$  in the exponent, and introducing the Dirac distribution

$$\int_{\mathbb{R}} dt \delta \left( t - \frac{\sum_{\alpha=1}^M e^{-i\hat{\Xi}_\alpha}}{M} \right) = 1 \quad (\text{D13})$$

yields

$$\mathcal{M}_{\vec{k},\chi} = \int_{\mathbb{R}^2} \frac{dt d\hat{t}}{2\pi} \prod_{j=1}^N \left( \int_0^{2\pi} \frac{d\hat{k}_j}{2\pi} e^{i\hat{k}_j k_j + \rho_* M t e^{-i\hat{k}_j/N}} \right) \prod_{\gamma=1}^M \left( \int_0^{2\pi} \frac{d\hat{\Xi}_\gamma}{2\pi} e^{i\hat{\Xi}_\gamma \chi + i\hat{t} e^{-i\hat{\Xi}_\gamma/M}} \right) e^{-i\hat{t} t} e^{-\rho_* M + \mathcal{O}_N(1)}. \quad (\text{D14})$$

We determine the integrals by expressing the exponentials in terms of their Taylor series,

$$\int_0^{2\pi} \frac{d\hat{k}_j}{2\pi} e^{i\hat{k}_j k_j + \rho_* M t e^{-i\hat{k}_j/N}} = \int_0^{2\pi} \frac{d\hat{k}_j}{2\pi} e^{i\hat{k}_j k_j} \sum_{\ell=0}^{\infty} \left( \frac{\rho_* M t}{N} \right)^\ell \frac{e^{-i\ell \hat{k}_j}}{\ell!} = \frac{(\rho_* M t)^{k_j}}{N^{k_j} k_j!}, \quad (\text{D15})$$

and analogously we get

$$\int_0^{2\pi} \frac{d\hat{\Xi}_\gamma}{2\pi} e^{i\hat{\Xi}_\gamma \chi + i\hat{t} e^{-i\hat{\Xi}_\gamma/M}} = \frac{(i\hat{t})^\chi}{M^\chi \chi!}. \quad (\text{D16})$$

Using the expressions (D15) and (D16) in Eq. (D14) gives

$$\mathcal{M}_{\vec{k},\chi} = \int_{\mathbb{R}^2} \frac{d\iota d\hat{\iota}}{2\pi} \left( \prod_{j=1}^N \frac{1}{k_j!} \right) \left[ \frac{\rho_* M \iota}{N} \right]^{\rho_* M} \left[ \frac{(i\hat{\iota})^\chi}{M \chi!} \right]^M e^{-i\hat{\iota}\iota - \rho_* M + \mathcal{O}_N(1)}. \quad (\text{D17})$$

Using  $M = \mu N$  and making the transformation  $\hat{\iota} \rightarrow \mu N \hat{\iota}$ , we get the saddle point integral

$$\mathcal{M}_{\vec{k},\chi} = \frac{\mu e^{-\rho_* M} N}{(\chi!)^M \prod_j k_j!} \int_{\mathbb{R}^2} \frac{d\iota d\hat{\iota}}{2\pi} e^{N\Psi(\iota, \hat{\iota}) + \mathcal{O}_N(1)} \quad (\text{D18})$$

with exponent

$$\Psi(\iota, \hat{\iota}) = -i\mu \hat{\iota} \iota + c \log \rho_* \mu \iota + \mu \chi \log i \hat{\iota}. \quad (\text{D19})$$

In the limit of  $N \rightarrow \infty$ , the saddle point dominates, and we get the expression

$$\mathcal{M}_{\vec{k},\chi} = \Phi_{\vec{k},\chi} e^{N\Psi(\iota^*, \hat{\iota}^*) + \mathcal{O}_N(1)}, \quad (\text{D20})$$

where  $\iota^*$  and  $\hat{\iota}^*$  solve the saddle point equation

$$i\mu \hat{\iota}^* \iota^* = c = \mu \chi, \quad (\text{D21})$$

and where

$$\Phi_{\vec{k},\chi} = \frac{\mu e^{-\rho_* M}}{(\chi!)^M \prod_j k_j!} \frac{1}{\sqrt{\det \mathcal{H}}} \quad (\text{D22})$$

with  $\mathcal{H}$  the Hessian of the function  $\Psi$  evaluated at the saddle point. Using Eq. (D21) in (D20) we obtain the final expression

$$\mathcal{M}_{\vec{k},\chi} = \Phi_{\vec{k},\chi} e^{Nc(\log \rho_* c - 1) + \mathcal{O}_N(1)}. \quad (\text{D23})$$

As will become evident, the prefactor  $\Phi_{\vec{k},\chi}$  cancels out with an identical prefactor that appears in the numerator of the derivation for  $\langle C_i^q(\mathbf{I}) \rangle_{\vec{k},\chi}$ , which we do in the next Section.

### b. Average clustering coefficient

Using the definition of the clustering coefficient, given by Eq. (13), and the fact that in this model all cardinalities are fixed to  $\chi$ , i.e.,  $\chi_\alpha = \chi$ , we get

$$\begin{aligned} \langle C_i^q(\mathbf{I}) \rangle_{\vec{k},\chi} &= \frac{2}{k_i(k_i-1)(\chi-1)} \left[ 1 - \frac{\sum_{i=1}^N (\delta_{0,k_i} + \delta_{1,k_i})}{N} \right] \\ &\times \frac{1}{\mathcal{M}_{\vec{k},\chi}} \sum_{\mathbf{I}} \sum_{\alpha, \beta, \alpha < \beta} \sum_{j=1; j \neq i}^N \delta_{\vec{k}, \vec{k}(\mathbf{I})} \delta_{\chi \vec{1}, \vec{\chi}(\mathbf{I})} I_{j\alpha} I_{j\beta} I_{i\alpha} I_{i\beta} \prod_{g=1}^N \prod_{\varepsilon=1}^M [p_* \delta_{I_{g\varepsilon}, 1} + (1-p_*) \delta_{I_{g\varepsilon}, 0}]. \end{aligned} \quad (\text{D24})$$

We represent the Kronecker delta functions in Eq. (D24) as integrals, and then sum over the  $\mathbf{I}$ -variables, yielding

$$\begin{aligned} \mathcal{M}_{\vec{k},\chi} \langle C_i^q(\mathbf{I}) \rangle &= \frac{2}{k_i(k_i-1)(\chi-1)} \left[ 1 - \frac{\sum_{i=1}^N (\delta_{0,k_i} + \delta_{1,k_i})}{N} \right] \int \prod_{n=1}^N \frac{d\hat{k}_n}{2\pi} e^{i\hat{k}_n k_n} \int \prod_{\xi=1}^M \frac{d\hat{\xi}_\xi}{2\pi} e^{j\hat{\xi}_\xi \chi} \\ &\times \sum_{\alpha, \beta; \alpha < \beta} \sum_{j=1; j \neq i}^N (p_*)^4 e^{-2i\hat{k}_i} e^{-2i\hat{k}_j} e^{-2i\hat{\xi}_\alpha} e^{-2i\hat{\xi}_\beta} \prod_{(g,\varepsilon)}' [p_* e^{-i\hat{k}_g} e^{-i\hat{\xi}_\varepsilon} + (1-p_*)], \end{aligned} \quad (\text{D25})$$

where  $\prod_{(g,\varepsilon)}'$  is a product over all pairs  $(g, \varepsilon) \in \mathcal{V} \times \mathcal{W}$ , but excluding  $\{(i, \alpha), (i, \beta), (j, \alpha), (j, \beta)\}$ . Setting  $p^* = \rho_*/N$  and taking the limit  $N \rightarrow \infty$ , we get for all  $g \notin \{i, j\}$  that

$$\prod_{\varepsilon=1}^M \left[ \frac{\rho_*}{N} e^{-i\hat{k}_g} e^{-i\hat{\xi}_\varepsilon} + (1 - \frac{\rho_*}{N}) \right] = \exp \left[ \rho_* M \frac{e^{-i\hat{k}_g}}{N} \frac{\sum_{\varepsilon=1}^M e^{-i\hat{\xi}_\varepsilon}}{M} - \frac{\rho_* M}{N} + \mathcal{O}(M/N^2) \right] \quad (\text{D26})$$

and for  $g \in \{i, j\}$  we get

$$\prod_{\substack{\varepsilon=1; \\ \varepsilon \neq \{\alpha, \beta\}}}^M \left[ \frac{\rho_*}{N} e^{-i\hat{k}_g} e^{-i\hat{\varepsilon}} + \left(1 - \frac{\rho_*}{N}\right) \right] = \exp \left[ \rho_* M \frac{e^{-i\hat{k}_g} \sum_{\varepsilon \notin \{\alpha, \beta\}} e^{-i\hat{\varepsilon}}}{N} - \frac{\rho_* (M-2)}{N} + \mathcal{O}(M/N^2) \right]. \quad (\text{D27})$$

Introducing

$$\int d\mathbf{t} \delta \left( \mathbf{t} - \frac{\sum_{\alpha=1}^M e^{-i\hat{\varepsilon}\alpha}}{M} \right) = 1 \quad (\text{D28})$$

this simplifies into

$$\begin{aligned} \mathcal{M}_{\vec{k}, \chi} \langle C_i^q(\mathbf{I}) \rangle &= \frac{2}{k_i(k_i-1)(\chi-1)} \left[ 1 - \frac{\sum_{i=1}^N (\delta_{0,k_i} + \delta_{1,k_i})}{N} \right] \int \frac{d\mathbf{t} d\hat{\mathbf{t}}}{2\pi} \sum_{\substack{\alpha, \beta; \\ \alpha < \beta}} \sum_{j=1; j \neq i}^N \prod_{i \neq 1}^N \left( \int \frac{d\hat{k}_n}{2\pi} e^{i\hat{k}_n k_n + \rho_* M \mathbf{t} e^{-i\hat{k}_n/N}} \right) \\ &\quad \times \prod_{\xi=1}^M \left( \int \frac{d\hat{\varepsilon}_\xi}{2\pi} e^{i\hat{\varepsilon}_\xi \chi + i\hat{\varepsilon}_\xi \mathbf{t} e^{-i\hat{\varepsilon}_\xi/M}} \right) \left( \frac{\rho_*}{N} \right)^4 e^{-2i\hat{k}_i} e^{-2i\hat{k}_j} e^{-2i\hat{\varepsilon}_\alpha} e^{-2i\hat{\varepsilon}_\beta} e^{-\rho_* M} e^{-i\hat{\mathbf{t}} + \mathcal{O}_N(1)}. \end{aligned}$$

Integrating over  $\hat{k}_n$  and  $\hat{\varepsilon}_\xi$  and using the formula

$$\int \frac{d\hat{k}_n}{2\pi} e^{i\hat{k}_n k_n + \rho_* M \mathbf{t} e^{-i\hat{k}_n/N}} = \int \frac{d\hat{k}_n}{2\pi} e^{i\hat{k}_n k_n} \sum_{\ell=0}^{\infty} \left( \frac{\rho_* M \mathbf{t}}{N} \right)^\ell \frac{e^{-i\ell \hat{k}_n}}{\ell!} = \frac{(\rho_* M \mathbf{t})^{k_n}}{N^{k_n} k_n!}$$

yields

$$\begin{aligned} \mathcal{M}_{\vec{k}, \chi} \langle C_i^q(\mathbf{I}) \rangle &= \frac{\mu N (\mu N - 1) \chi^2 (\chi - 1)}{(\chi!)^M \prod_j k_j!} \left[ 1 - \frac{\sum_{i=1}^N (\delta_{0,k_i} + \delta_{1,k_i})}{N} \right] \int \frac{d\mathbf{t} d\hat{\mathbf{t}}}{2\pi} \\ &\quad \times \sum_{j=1; j \neq i}^N \left( \frac{\rho_*}{N} \right)^4 k_j (k_j - 1) e^{-\rho_* M} e^{-i\hat{\mathbf{t}} \mathbf{t}} \left( \frac{\rho_* M \mathbf{t}}{N} \right)^{\rho_* M - 4} \left( \frac{i\hat{\mathbf{t}}}{M} \right)^{M\chi - 4} e^{\mathcal{O}_N(1)}. \end{aligned}$$

After the transformation  $\hat{\mathbf{t}} \rightarrow \mu N \hat{\mathbf{t}}$ , we can write this expression as the following saddle point integral

$$\mathcal{M}_{\vec{k}, \chi} \langle C_i^q(\mathbf{I}) \rangle = \frac{\mu^3 \chi^2 (\chi - 1) e^{-\rho_* M}}{N (\chi!)^M \prod_j k_j!} \left[ 1 - \frac{\sum_{i=1}^N (\delta_{0,k_i} + \delta_{1,k_i})}{N} \right] \sum_{\substack{j=1; \\ j \neq i}}^N k_j (k_j - 1) \int \frac{d\mathbf{t} d\hat{\mathbf{t}}}{2\pi} \frac{e^{N\Psi(\mathbf{t}, \hat{\mathbf{t}}) + \mathcal{O}_N(1)}}{(\mu i \hat{\mathbf{t}})^4} \quad (\text{D29})$$

where  $\Psi(\mathbf{t}, \hat{\mathbf{t}})$  is given by Eq. (D19).

In the limit of  $N \rightarrow \infty$ , the saddle point dominates. However, since the exponent is identical to the one appearing in Eq. (D18) for  $\mathcal{M}_{\vec{k}, \chi}$ , we get the simpler expression

$$\begin{aligned} \langle C_i^q(\mathbf{I}) \rangle &= \frac{\chi - 1}{(N\mu\chi)^2} \left[ 1 - \frac{\sum_{i=1}^N (\delta_{0,k_i} + \delta_{1,k_i})}{N} \right] \sum_{j=1; j \neq i}^N k_j (k_j - 1) + \mathcal{O} \left( \frac{1}{N^2} \right) \\ &= \frac{\chi - 1}{\bar{k}^2 N} k(k-1) (1 - p_{\text{deg}}(0) - p_{\text{deg}}(1)) + \mathcal{O} \left( \frac{1}{N^2} \right), \quad (\text{D30}) \end{aligned}$$

which is identical to Eq. (36) in the main text. A comparison between Eq. (D30) and the average quad clustering coefficient of large numerically generated random graphs shows an excellent agreement (results not shown).

If all terms of the degree sequence are equal (i.e., it is  $(c, \chi)$ -regular hypergraph), then Eq. (D30) becomes  $\langle C_i^q(\mathbf{I}) \rangle = (c - 1)(\chi - 1)/(cN) + \mathcal{O}(1/N^2)$ .

## Appendix E: Average quad clustering coefficient for biregular cardinalities

We obtain the Eq. (41) for the ensemble averaged quad clustering coefficient of the model (39) with biregular cardinalities.



**a. Normalisation constant of  $P_{\chi_1, \chi_2}$**

By assumption, there are  $M_1$  hyperedges with cardinality  $\chi_1$  and  $M_2 = M - M_1$  hyperedges with cardinality  $\chi_2$ . The hyperedges and nodes are connected randomly, given their prescribed cardinalities. Therefore, the normalisation constant in Eq. (39) is given by

$$\mathcal{N}_{\chi_1, \chi_2} = \sum_{\mathbf{I}} \prod_{\alpha=1}^{M_1} \delta_{\chi_1, \chi_\alpha(\mathbf{I})} \prod_{\beta=M_1+1}^M \delta_{\chi_2, \chi_\beta(\mathbf{I})} = \left[ \binom{N}{\chi_1} \right]^{M_1} \left[ \binom{N}{\chi_2} \right]^{M_2}. \quad (\text{E1})$$

**b. Average clustering coefficient**

Using the definition of the clustering coefficient, Eq. (13), in the definition of the average clustering coefficient, Eq. (40), yields

$$\begin{aligned} \mathcal{N}_{\chi_1, \chi_2} \langle C_{q,i}(\mathbf{I}) \rangle_{\chi_1, \chi_2} &= \sum_{u=0}^{M_1} \sum_{v=0}^{M_2} \frac{2}{(\chi_1 - 1)(u+v)(u+v-1) + v(\chi_2 - \chi_1)(v-1)} \\ &\quad \times \sum_{\alpha, \beta, \alpha < \beta} \sum_{j=1; j \neq i}^N \sum_{\mathbf{I}} \delta_{u, k_i(\mathbf{I}; \chi_1)} \delta_{v, k_i(\mathbf{I}; \chi_2)} \prod_{\varepsilon_1=1}^{M_1} \delta_{\chi_1, \chi_{\varepsilon_1}(\mathbf{I})} \prod_{\varepsilon_2=M_1+1}^M \delta_{\chi_2, \chi_{\varepsilon_2}(\mathbf{I})} I_{j\alpha} I_{j\beta} I_{i\alpha} I_{i\beta}. \end{aligned} \quad (\text{E2})$$

Representing the Kronecker delta functions with integrals, we get

$$\begin{aligned} \mathcal{N}_{\chi_1, \chi_2} \langle C_i^q(\mathbf{I}) \rangle_{\chi_1, \chi_2} &= \sum_{u=0}^{M_1} \sum_{v=0}^{M_2} \sum_{\hat{q} \in \mathbb{N}^N} \frac{2}{(\chi_1 - 1)(u+v)(u+v-1) + v(\chi_2 - \chi_1)(v-1)} \\ &\quad \times \int_0^{2\pi} \frac{d\hat{u}}{2\pi} e^{i\hat{u}u} \int_0^{2\pi} \frac{d\hat{v}}{2\pi} e^{i\hat{v}v} \int_{[0, 2\pi]^N} \prod_{n=1}^N \frac{d\hat{q}_n}{2\pi} e^{i\hat{q}_n q_n} \int_{[0, 2\pi]^{M_1}} \prod_{\xi=1}^{M_1} \frac{d\hat{\xi}_\xi}{2\pi} e^{i\hat{\xi}_\xi \chi_1} \int_{[0, 2\pi]^{M_2}} \prod_{\xi=M_1+1}^M \frac{d\hat{\xi}_\xi}{2\pi} e^{i\hat{\xi}_\xi \chi_2} \\ &\quad \times \sum_{\alpha, \beta, \alpha < \beta} \sum_{j=1; j \neq i}^N \sum_{\mathbf{I}} e^{-i\hat{u} \sum_{\gamma} I_{i\gamma} \delta_{\chi_1, \chi_\gamma(\mathbf{I})}} e^{-i\hat{v} \sum_{\gamma} I_{i\gamma} \delta_{\chi_2, \chi_\gamma(\mathbf{I})}} \prod_{n'=1}^N e^{-i\hat{q}_{n'} \sum_{\mu} I_{n'\mu}} \prod_{\xi'=1}^M e^{-i\hat{\xi}_{\xi'} \sum_{o} I_{o\xi'} I_{j\alpha} I_{j\beta} I_{i\alpha} I_{i\beta}}. \end{aligned} \quad (\text{E3})$$

Summing over the  $\mathbf{I}$  variables, and subsequently integrating over the  $\hat{q}_n$  and  $\hat{\xi}_\xi$  variables, we get the expression

$$\begin{aligned} \mathcal{N}_{\chi_1, \chi_2} \langle C_i^q(\mathbf{I}) \rangle_{\chi_1, \chi_2} &= \sum_{u=0}^{M_1} \sum_{v=0}^{M_2} \frac{2(N-1)}{(\chi_1 - 1)(u+v)(u+v-1) + v(\chi_2 - \chi_1)(v-1)} \int_0^{2\pi} \frac{d\hat{u}}{2\pi} e^{i\hat{u}u} \int_0^{2\pi} \frac{d\hat{v}}{2\pi} e^{i\hat{v}v} \\ &\quad \times [(p_*)^{\chi_\alpha} (1-p_*)^{N-\chi_\alpha}]^{M_1} [(p_*)^{\chi_2} (1-p_*)^{N-\chi_2}]^{M_2} \\ &\quad \times \left\{ \left[ \binom{M_1}{2} \left( \left( \frac{N-2}{\chi_1-2} e^{-\hat{u}} \right)^2 \left( \frac{N-1}{\chi_1-1} e^{-i\hat{u}} + \frac{N-1}{\chi_1} \right) \right)^{M_1-2} \left( \frac{N-1}{\chi_2-1} e^{-i\hat{v}} + \frac{N-1}{\chi_2} \right)^{M_2} \right. \right. \\ &\quad \left. \left. + \binom{M_1}{1} \binom{M_2}{1} \left( \frac{N-2}{\chi_1-2} e^{-\hat{u}} \right) \left( \frac{N-2}{\chi_2-2} e^{-\hat{v}} \right) \left( \frac{N-1}{\chi_1-1} e^{-i\hat{u}} + \frac{N-1}{\chi_1} \right)^{M_1-1} \left( \frac{N-1}{\chi_2-1} e^{-i\hat{v}} + \frac{N-1}{\chi_2} \right)^{M_2-1} \right. \right. \\ &\quad \left. \left. + \binom{M_2}{2} \left( \left( \frac{N-2}{\chi_2-2} e^{-\hat{v}} \right)^2 \left( \frac{N-1}{\chi_1-1} e^{-i\hat{u}} + \frac{N-1}{\chi_1} \right) \right)^{M_1} \left( \frac{N-1}{\chi_2-1} e^{-i\hat{v}} + \frac{N-1}{\chi_2} \right)^{M_2-2} \right] \right\}. \end{aligned} \quad (\text{E4})$$

Lastly, integrating over the variables  $\hat{u}$  and  $\hat{v}$  yields

$$\begin{aligned}
\mathcal{N}_{\chi_1, \chi_2} \langle C_i^q(\mathbf{I}) \rangle_{\chi_1, \chi_2} &= \sum_{u=2}^{M_1} \sum_{v=0}^{M_2} \frac{2(N-1) [(p_*)^{\chi_1} (1-p_*)^{N-\chi_1}]^{M_1} [(p_*)^{\chi_2} (1-p_*)^{N-\chi_2}]^{M_2}}{(\chi_1-1)(u+v)(u+v-1) + v(\chi_2-\chi_1)(v-1)} \\
&\times \binom{M_1}{2} \left[ \binom{N-2}{\chi_1-2} \right]^2 \binom{M_1-2}{u-2} \left[ \binom{N-1}{\chi_1-1} \right]^{u-2} \left[ \binom{N-1}{\chi_1} \right]^{M_1-u} \binom{M_2}{v} \left[ \binom{N-1}{\chi_2-1} \right]^v \left[ \binom{N-1}{\chi_2} \right]^{M_2-v} \\
&\quad + \sum_{u=1}^{M_1} \sum_{v=1}^{M_2} \frac{2(N-1) [(p_*)^{\chi_1} (1-p_*)^{N-\chi_1}]^{M_1} [(p_*)^{\chi_2} (1-p_*)^{N-\chi_2}]^{M_2}}{(\chi_1-1)(u+v)(u+v-1) + v(\chi_2-\chi_1)(v-1)} \\
&\times M_1 M_2 \binom{N-2}{\chi_1-2} \binom{N-2}{\chi_2-2} \binom{M_1-1}{u-1} \left[ \binom{N-1}{\chi_1-1} \right]^{u-1} \left[ \binom{N-1}{\chi_1} \right]^{M_1-u} \binom{M_2-1}{v-1} \left[ \binom{N-1}{\chi_2-1} \right]^{v-1} \left[ \binom{N-1}{\chi_2} \right]^{M_2-v} \\
&\quad + \sum_{u=0}^{M_1} \sum_{v=2}^{M_2} \frac{2(N-1) [(p_*)^{\chi_1} (1-p_*)^{N-\chi_1}]^{M_1} [(p_*)^{\chi_2} (1-p_*)^{N-\chi_2}]^{M_2}}{(\chi_1-1)(u+v)(u+v-1) + v(\chi_2-\chi_1)(v-1)} \\
&\times \binom{M_2}{2} \left[ \binom{N-2}{\chi_2-2} \right]^2 \binom{M_1}{u} \left[ \binom{N-1}{\chi_1-1} \right]^u \left[ \binom{N-1}{\chi_1} \right]^{M_1-u} \binom{M_2-2}{v-2} \left[ \binom{N-1}{\chi_2-1} \right]^{v-2} \left[ \binom{N-1}{\chi_2} \right]^{M_2-v}, \quad (\text{E5})
\end{aligned}$$

which gives the Eqs. (41-43) in the main text after dividing by the expression (E1) for the normalisation constant.

## Appendix F: Datasets for real-world hypergraphs

In Secs. V and VI of this Paper, we have considered six nondirected hypergraphs. These are:

1. *NDC-substances*<sup>28</sup>: The nodes are substances, and the hyperedges are commercial drugs registered in by the U.S. Food and Drug Administration in the National Drug Code (NDC). A node is linked to a hyperedge whenever the corresponding substance is used to synthesise the drug.
2. *Youtube*<sup>29,30</sup>: Nodes represent YouTube users and hyperedges represent Youtube channels with paid subscription. A user is linked to a hyperedge when the user pays for the membership service.
3. *Food recipe*<sup>31</sup>: Nodes are ingredients and hyperedges are recipes for food dishes.
4. *Github*<sup>29,32</sup>: Nodes are GitHub users and hyperedges are GitHub projects. A node is linked to a hyperedge whenever the corresponding user contributes to the GitHub project.
5. *Crime involvement*<sup>29</sup>: The nodes are suspects, and the hyperedges are crime cases. Nodes are linked to hyperedges whenever the corresponding suspects are involved with the crime investigation.
6. *Walmart*<sup>33</sup>: Nodes are products sold by Walmart, and the hyperedges represent purchase orders. Nodes are linked to hyperedges whenever the corresponding products are part of the purchased order.

In Sec. VID, we have considered three directed hypergraphs:

1. *DNC-email*<sup>29</sup>: Nodes are users sending and receiving emails and hyperedges are emails that are part of the 2016 Democratic National Committee (DNC) email leak. Hyperedges are directed from the sender to its recipients. Since an email always has a single sender, all hyperedges have an in-cardinality equal to one.
2. *Human metabolic pathways*<sup>35</sup>: Nodes represent metabolic compounds in the human metabolism, and hyperedges are metabolic reactions. A hyperedge is directed from the reactants towards the products of the metabolic reaction, and metabolic reactions with very small rates are omitted, yielding a directed hypergraph.
3. *English thesaurus*<sup>34</sup>: Nodes are English words and hyperedges represent synonym relations between words. Hyperedges are directed from a root word to target words. Since not all words occur as root words, the hypergraph is directed. The in-cardinality of each hyperedge equals to one.

### Appendix G: Configuration model for hypergraphs

We describe the algorithm used to generate a single instance from the configuration model for hypergraphs. There are two type of configuration models: the microcanonical ensemble that specifies the degree  $\vec{k}(\mathbf{I})$  and cardinality  $\vec{\chi}(\mathbf{I})$  sequences and the canonical ensemble that specifies the distributions  $P(k)$  and  $P(\chi)$  for the degrees and cardinalities of nodes and hyperedges, respectively. In the microcanonical ensemble links are generated randomly between nodes and hyperedges given the specified sequences, while in the canonical ensemble we first generate these sequences, and then generate the links.

In Section V and VI, we use a micro-canonical ensemble with the number of nodes  $N$ , hyperedges  $M$ , degree sequence  $\vec{k}$ , and the cardinality sequence  $\vec{\chi}$  as given by the real-world hypergraph under study. The links between the nodes and hyperedges are generated as follows. We associate a number of stubs to the nodes and hyperedges of the graph corresponding to their degrees and cardinalities. Subsequently, we randomly connect the stubs of nodes with those of hyperedges with the additional constraints that there are no multiple links connecting the same pair of nodes and hyperedges. The upper Panel of Fig. 15 shows an example of this process for the case of  $\vec{k} = (1, 1, 1, 2, 2, 1, 1, 1)$  and  $\vec{\chi} = (5, 5)$ . An analogous process applies to directed hypergraphs and is illustrated in the lower Panel of Fig. 15 for  $\vec{k}_i^{\text{in}} = (0, 0, 0, 1, 1, 1, 1, 1)$ ,  $\vec{k}^{\text{out}} = (1, 1, 1, 1, 1, 1, 0)$ ,  $\vec{\chi}^{\text{in}} = \{3, 4\}$  and  $\vec{\chi}^{\text{out}} = \{2, 3\}$ .

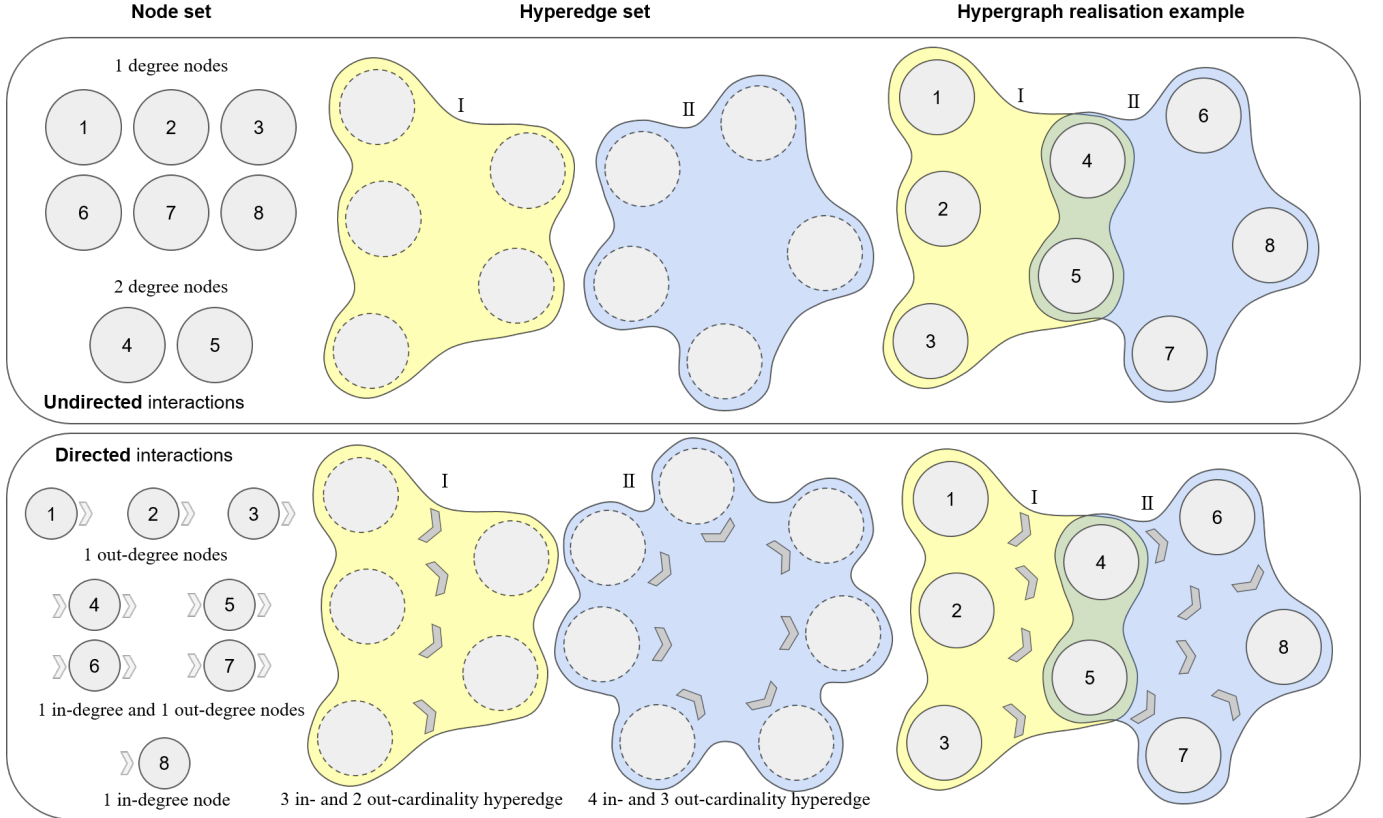


FIG. 15: Example of two sets of nodes and hyperedges with their stubs (one nondirected and another one directed), and an example of two random hypergraphs generated from these initial configurations.

### Appendix H: Denominator of the quad clustering coefficient for a directed hypergraphs

In this Appendix, we provide an explicit expression for the maximum number of directed quads,  $q_{\text{max}}^{\leftrightarrow}(\{\mathcal{X}_{i\alpha}(\mathbf{I}^{\leftrightarrow}), I_{i\alpha}^{\leftrightarrow}\}_{\alpha \in \mathcal{D}_i})$ , that a node  $i$  can have when it is connected to a set of hyperedges  $\alpha \in \mathcal{D}_i$  for which (i) the cardinalities of the hyperedges  $\alpha$  are given by those in the sets  $\mathcal{X}_{i\alpha} = \{\chi_{\alpha,i}^{\text{in}}(\mathbf{I}^{\leftrightarrow}), \chi_{\alpha,i}^{\text{out}}(\mathbf{I}^{\leftrightarrow})\}$  and (ii) the symmetry of the links connecting node  $i$  to the hyperedges  $\alpha$  are determined by the values  $I_{i\alpha}^{\leftrightarrow}$ . The expression for  $q_{\text{max}}^{\leftrightarrow}$  can be decomposed into

$$q_{\text{max}}^{\leftrightarrow}(\{\mathcal{X}_{i\alpha}(\mathbf{I}^{\leftrightarrow}), I_{i\alpha}^{\leftrightarrow}\}_{\alpha \in \mathcal{D}_i}) \equiv \sum_{\alpha, \beta; \alpha < \beta} (\mathbf{I}^{\leftrightarrow})_{i\alpha}(\mathbf{I}^{\leftrightarrow})_{i\beta} \mathcal{W}(\mathcal{X}_{i\alpha}(\mathbf{I}^{\leftrightarrow}), \mathcal{X}_{i\beta}(\mathbf{I}^{\leftrightarrow})), \quad (\text{H1})$$

where  $\mathcal{W}$  is an integer valued function that is independent of the symmetry of the links  $(i, \alpha)$  and  $(i, \beta)$  (as determined by  $\mathbf{I}_{i\alpha}^{\leftrightarrow}$  and  $\mathbf{I}_{i\beta}^{\leftrightarrow}$ ). In what follows we specify  $\mathcal{W}(\mathcal{X}_{i\alpha}, \mathcal{X}_{i\beta})$  for the four possible scenarios, viz., (1)  $\chi_{\alpha,i}^{\text{in}} = \chi_{\alpha,i}^{\text{out}}$  and  $\chi_{\beta,i}^{\text{in}} = \chi_{\beta,i}^{\text{out}}$  (see Appendix H 1); (2)  $\chi_{\alpha,i}^{\text{in}} = \chi_{\alpha,i}^{\text{out}}$  and  $\chi_{\beta,i}^{\text{in}} \neq \chi_{\beta,i}^{\text{out}}$ , or  $\chi_{\alpha,i}^{\text{in}} \neq \chi_{\alpha,i}^{\text{out}}$  and  $\chi_{\beta,i}^{\text{in}} = \chi_{\beta,i}^{\text{out}}$  (see Appendix H 2); (3)  $\chi_{\alpha,i}^{\text{in}} \neq \chi_{\alpha,i}^{\text{out}}$  and  $\chi_{\beta,i}^{\text{in}} \neq \chi_{\beta,i}^{\text{out}}$ . Additionally,  $|\mathcal{X}_{i\alpha} \cup \mathcal{X}_{i\beta}| \neq 4$  (see Appendix H 3); (4)  $\chi_{\alpha,i}^{\text{in}} \neq \chi_{\alpha,i}^{\text{out}}$  and  $\chi_{\beta,i}^{\text{in}} \neq \chi_{\beta,i}^{\text{out}}$ . Additionally,  $|\mathcal{X}_{i\alpha} \cup \mathcal{X}_{i\beta}| = 4$  (see Appendix H 4).

1.  $\chi_{\alpha,i}^{\text{in}} = \chi_{\alpha,i}^{\text{out}}$  and  $\chi_{\beta,i}^{\text{in}} = \chi_{\beta,i}^{\text{out}}$

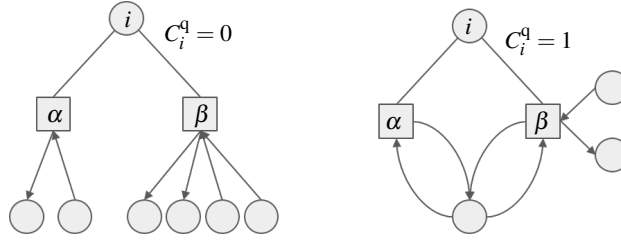


FIG. 16: Two motifs consisting of a node  $i$  linked with two hyperedges  $\alpha$  and  $\beta$  and for which  $\chi_{\alpha,i}^{\text{in}} = \chi_{\alpha,i}^{\text{out}} = 1$  and  $\chi_{\beta,i}^{\text{in}} = \chi_{\beta,i}^{\text{out}} = 2$ , corresponding with Appendix H 1. Left panel shows an example with  $C_i^q = 0$  and the right panel has  $C_i^q = 1$ .

In this case

$$\mathcal{W}(\mathcal{X}_{i\alpha}(\mathbf{I}^{\leftrightarrow}), \mathcal{X}_{i\beta}(\mathbf{I}^{\leftrightarrow})) \equiv 4 \min(|\mathcal{X}_{i\alpha}(\mathbf{I}^{\leftrightarrow}) \cup \mathcal{X}_{i\beta}(\mathbf{I}^{\leftrightarrow})|). \quad (\text{H2})$$

Figure 16 shows two examples, one for which  $C_i^q = 0$  and another one for which  $C_i^q = 1$ .

2.  $\chi_{\alpha,i}^{\text{in}} = \chi_{\alpha,i}^{\text{out}}$  and  $\chi_{\beta,i}^{\text{in}} \neq \chi_{\beta,i}^{\text{out}}$

We define the minimum cardinality by  $\chi_{\min} \equiv \min(\{\chi_{\alpha,i}^{\text{in}}, \chi_{\beta,i}^{\text{in}}, \chi_{\beta,i}^{\text{out}}\})$  and the maximum value by  $\chi_{\max} \equiv \max(\{\chi_{\alpha,i}^{\text{in}}, \chi_{\beta,i}^{\text{in}}, \chi_{\beta,i}^{\text{out}}\})$ . In case the three values  $\chi_{\alpha,i}^{\text{in}}$ ,  $\chi_{\beta,i}^{\text{in}}$  and  $\chi_{\beta,i}^{\text{out}}$  are distinct, we use the notation  $\chi_{\text{med}}$  for the median value. Using this notation, we can express

$$\mathcal{W}(\mathcal{X}_{i\alpha}, \mathcal{X}_{i\beta}) \equiv \begin{cases} 4\chi_{\min}, & \text{if } \min(|\mathcal{X}_{i\alpha} \cup \mathcal{X}_{i\beta}|) = \chi_{\alpha,i}^{\text{in}}, \\ 2\chi_{\min} + 2\chi_{\text{med}}, & \text{if } \min(|\mathcal{X}_{i\alpha} \cup \mathcal{X}_{i\beta}|) \neq \chi_{\alpha,i}^{\text{in}} \text{ and } |\mathcal{X}_{i\alpha} \cup \mathcal{X}_{i\beta}| = 3, \\ 2\chi_{\min} + 2\chi_{\max}, & \text{otherwise.} \end{cases} \quad (\text{H3})$$

Fig. 17 shows examples with  $C_i^q = 0$  and  $C_i^q = 1$  for each the three above cases.

For the case with  $\chi_{\alpha,i}^{\text{in}} \neq \chi_{\alpha,i}^{\text{out}}$  and  $\chi_{\beta,i}^{\text{in}} = \chi_{\beta,i}^{\text{out}}$  an analogous expression applies with the two indices  $\alpha$  and  $\beta$  swapped.

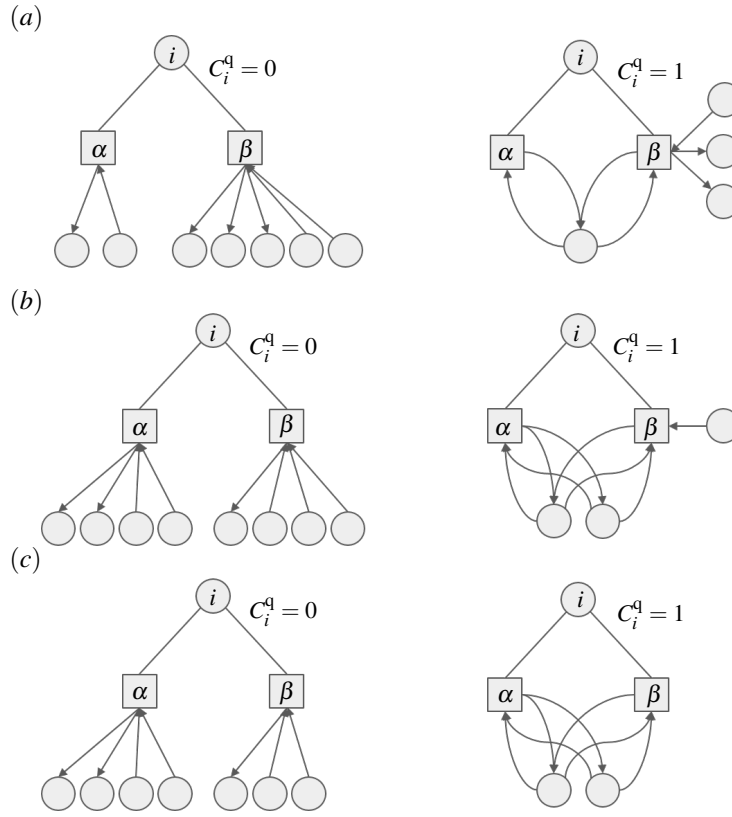


FIG. 17: Motifs consisting of a node  $i$  linked with two hyperedges  $\alpha$  and  $\beta$  and for which  $\chi_{\alpha,i}^{\text{in}} = \chi_{\alpha,i}^{\text{out}}$  and  $\chi_{\beta,i}^{\text{in}} \neq \chi_{\beta,i}^{\text{out}}$ , corresponding with Appendix H 2. Left panels show examples with  $C_i^q = 0$  and for the right panels  $C_i^q = 1$ . Panels (a)-(c) correspond with the different cases in Eq. (H3). Panel (a):  $\chi_{\alpha,i}^{\text{in}} = \chi_{\alpha,i}^{\text{out}} = 1$ ,  $\chi_{\beta,i}^{\text{in}} = 2$ , and  $\chi_{\beta,i}^{\text{out}} = 3$ . Panel (b):  $\chi_{\alpha,i}^{\text{in}} = \chi_{\alpha,i}^{\text{out}} = 2$ ,  $\chi_{\beta,i}^{\text{in}} = 3$ , and  $\chi_{\beta,i}^{\text{out}} = 1$ . Panel (c):  $\chi_{\alpha,i}^{\text{in}} = \chi_{\alpha,i}^{\text{out}} = 2$ ,  $\chi_{\beta,i}^{\text{in}} = 2$ , and  $\chi_{\beta,i}^{\text{out}} = 1$ .

3.  $\chi_{\alpha,i}^{\text{in}} \neq \chi_{\alpha,i}^{\text{out}}$ ,  $\chi_{\beta,i}^{\text{in}} \neq \chi_{\beta,i}^{\text{out}}$ , and  $|\mathcal{X}_{i\alpha} \cup \mathcal{X}_{i\beta}| \neq 4$ .

As in Appendix H 2, we use the notation  $\chi_{\min} \equiv \min(\{\chi_{\alpha,i}^{\text{in}}, \chi_{\alpha,i}^{\text{out}}, \chi_{\beta,i}^{\text{in}}, \chi_{\beta,i}^{\text{out}}\})$  and  $\chi_{\max} \equiv \max(\{\chi_{\alpha,i}^{\text{in}}, \chi_{\alpha,i}^{\text{out}}, \chi_{\beta,i}^{\text{in}}, \chi_{\beta,i}^{\text{out}}\})$ . In addition, if  $|\mathcal{X}_{i\alpha} \cup \mathcal{X}_{i\beta}| = 3$ , then a third median value exists, which we denote by  $\chi_{\text{med}}$ . Using this notation, we get

$$\mathcal{W}(\mathcal{X}_{i\alpha}, \mathcal{X}_{i\beta}) \equiv \begin{cases} 3\chi_{\min} + \chi_{\max}, & \text{if } |\mathcal{X}_{i\alpha} \cup \mathcal{X}_{i\beta}| = 2, \\ 3\chi_{\min} + \chi_{\text{med}}, & \text{if } |\mathcal{X}_{i\alpha} \cup \mathcal{X}_{i\beta}| = 3 \text{ and } \min(\mathcal{X}_{i\alpha}) = \min(\mathcal{X}_{i\beta}), \\ 2\chi_{\min} + 2\chi_{\text{med}}, & \text{if } |\mathcal{X}_{i\alpha} \cup \mathcal{X}_{i\beta}| = 3 \text{ and either } \max(\mathcal{X}_{i\alpha}) = \min(\mathcal{X}_{i\beta}) \text{ or } \max(\mathcal{X}_{i\beta}) = \min(\mathcal{X}_{i\alpha}), \\ 2\chi_{\min} + \chi_{\max} + \chi_{\text{med}}, & \text{if } |\mathcal{X}_{i\alpha} \cup \mathcal{X}_{i\beta}| = 3 \text{ and } \max(\mathcal{X}_{i\alpha}) = \max(\mathcal{X}_{i\beta}). \end{cases} \quad (\text{H4})$$

Fig. 18 shows examples with  $C_i^q = 0$  or  $C_i^q = 1$  for each of the four cases mentioned in formula (H4).

4.  $\chi_{\alpha,i}^{\text{in}} \neq \chi_{\alpha,i}^{\text{out}}$ ,  $\chi_{\beta,i}^{\text{in}} \neq \chi_{\beta,i}^{\text{out}}$ , and  $|\mathcal{X}_{i\alpha} \cup \mathcal{X}_{i\beta}| = 4$ .

In this case, the four cardinalities in the set  $\{\chi_{\alpha,i}^{\text{in}}, \chi_{\alpha,i}^{\text{out}}, \chi_{\beta,i}^{\text{in}}, \chi_{\beta,i}^{\text{out}}\}$  are all different. We order them from small to large and use the notation  $\chi_{\text{smallest}} < \chi_{\text{small}} < \chi_{\text{large}} < \chi_{\text{largest}}$  so that  $\chi_{\text{smallest}} \equiv \min(\{\chi_{\alpha,i}^{\text{in}}, \chi_{\alpha,i}^{\text{out}}, \chi_{\beta,i}^{\text{in}}, \chi_{\beta,i}^{\text{out}}\})$ , and so forth. The expression for

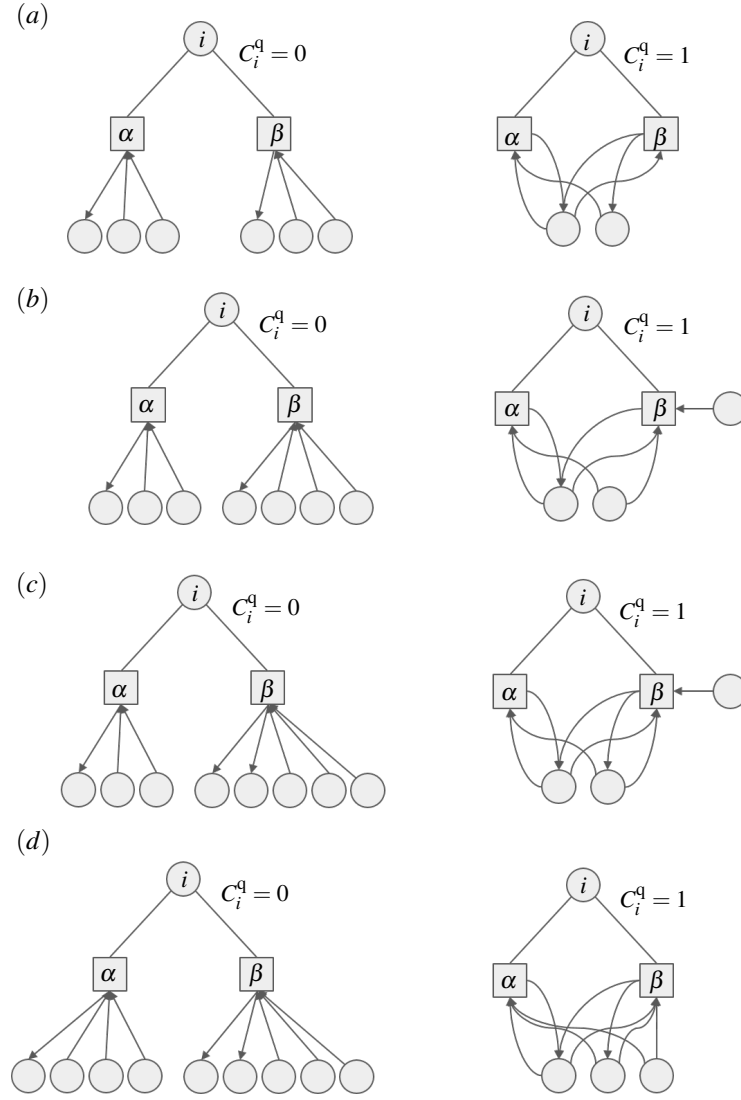


FIG. 18: Motifs consisting of a node  $i$  linked with two hyperedges  $\alpha$  and  $\beta$  and for which  $\chi_{\alpha,i}^{\text{in}} \neq \chi_{\alpha,i}^{\text{out}}$ ,  $\chi_{\beta,i}^{\text{in}} \neq \chi_{\beta,i}^{\text{out}}$ , and  $|\mathcal{X}_{i\alpha} \cup \mathcal{X}_{i\beta}| \neq 4$ , corresponding with Appendix H 3. Left panels show examples with  $C_i^q = 0$  and the right panels have  $C_i^q = 1$ . Left panels show examples with  $C_i^q = 0$  and for the right panels  $C_i^q = 1$ . Panels (a)-(d) correspond with the different cases in Eq. (H4). Panel (a):  $\chi_{\alpha,i}^{\text{in}} = 2$ ,  $\chi_{\alpha,i}^{\text{out}} = 1$ ,  $\chi_{\beta,i}^{\text{in}} = 2$ , and  $\chi_{\beta,i}^{\text{out}} = 1$ . Panel (b):  $\chi_{\alpha,i}^{\text{in}} = 2$ ,  $\chi_{\alpha,i}^{\text{out}} = 1$ ,  $\chi_{\beta,i}^{\text{in}} = 3$ , and  $\chi_{\beta,i}^{\text{out}} = 1$ . Panel (c):  $\chi_{\alpha,i}^{\text{in}} = 2$ ,  $\chi_{\alpha,i}^{\text{out}} = 1$ ,  $\chi_{\beta,i}^{\text{in}} = 3$ , and  $\chi_{\beta,i}^{\text{out}} = 2$ . Panel (d):  $\chi_{\alpha,i}^{\text{in}} = 3$ ,  $\chi_{\alpha,i}^{\text{out}} = 1$ ,  $\chi_{\beta,i}^{\text{in}} = 3$ , and  $\chi_{\beta,i}^{\text{out}} = 2$ .

$\mathcal{W}$  takes then the form

$$\mathcal{W}(\mathcal{X}_{i\alpha}, \mathcal{X}_{i\beta}) \equiv \begin{cases} 2\chi_{\text{smallest}} + 2\chi_{\text{small}}, & \text{if } \max(\mathcal{X}_{i\alpha}) < \min(\mathcal{X}_{i\beta}) \text{ or } \min(\mathcal{X}_{i\alpha}) > \max(\mathcal{X}_{i\beta}), \\ 2\chi_{\text{smallest}} + \chi_{\text{large}} + \chi_{\text{small}}, & \text{otherwise.} \end{cases} \quad (\text{H5})$$

Fig. 19 shows the examples of  $C_i^q = 0$  and  $C_i^q = 1$  for both cases in Eq. (H5).

#### Appendix I: For nondirected hypergraphs $C_i^{q\leftrightarrow}(\mathbf{I}^{\leftrightarrow}) = C_i^q(\mathbf{I})$

For a nondirected hypergraph  $\mathbf{I}^{\rightarrow} = \mathbf{I}^{\leftarrow} = \mathbf{I}$ , such that (67) reads

$$C_i^{q\leftrightarrow}(\mathbf{I}^{\leftrightarrow}) = 4 \frac{\sum_{j,j \neq i} \sum_{\alpha, \beta; \alpha < \beta} I_{i\alpha} I_{j\alpha} I_{i\beta} I_{j\beta}}{\sum_{\alpha, \beta; \alpha < \beta} I_{i\alpha} I_{i\beta} \mathcal{W}(\mathcal{X}_{i\alpha}, \mathcal{X}_{i\beta})}. \quad (\text{I1})$$

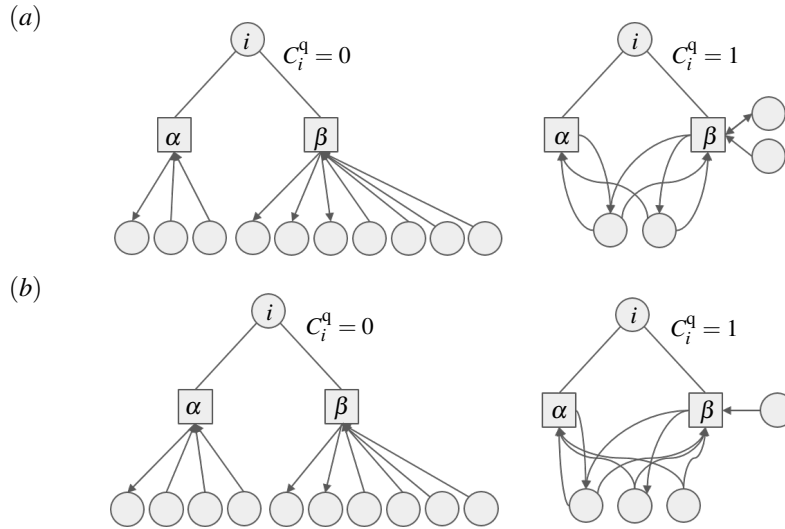


FIG. 19: Motifs consisting of a node  $i$  linked with two hyperedges  $\alpha$  and  $\beta$  and for which  $\chi_{\alpha,i}^{\text{in}} \neq \chi_{\alpha,i}^{\text{out}}$ ,  $\chi_{\beta,i}^{\text{in}} \neq \chi_{\beta,i}^{\text{out}}$ , and  $|\mathcal{X}_{i\alpha} \cup \mathcal{X}_{i\beta}| = 4$ , corresponding with Appendix H 4. Left panels show examples with  $C_i^q = 0$  and the right panels have  $C_i^q = 1$ . Panels (a)-(b) correspond with the two different cases in Eq. (H5). Panel (a):  $\chi_{\alpha,i}^{\text{in}} = 2$ ,  $\chi_{\alpha,i}^{\text{out}} = 1$ ,  $\chi_{\beta,i}^{\text{in}} = 4$ , and  $\chi_{\beta,i}^{\text{out}} = 3$ . Panel (b):  $\chi_{\alpha,i}^{\text{in}} = 3$ ,  $\chi_{\alpha,i}^{\text{out}} = 1$ ,  $\chi_{\beta,i}^{\text{in}} = 4$ , and  $\chi_{\beta,i}^{\text{out}} = 2$ .

Furthermore, as the hypergraph is nondirected,  $\chi_{\alpha,i}^{\text{in}} = \chi_{\alpha,i}^{\text{out}}$  and  $\chi_{\beta,i}^{\text{in}} = \chi_{\beta,i}^{\text{out}}$ , and hence the case of Appendix H 1 applies for  $\mathcal{W}$  and its expression is given by Eq. (H2). Using this formula we obtain

$$C_i^{q\leftrightarrow}(\mathbf{I}) = \frac{4 \sum_{j,j \neq i} \sum_{\alpha,\beta:\alpha < \beta} I_{i\alpha} I_{j\alpha} I_{i\beta} I_{j\beta}}{\sum_{\alpha,\beta:\alpha < \beta} (I_{i\alpha} I_{i\beta}) 4 \min \{ (\sum_{j,i \neq j} I_{j\alpha}), (\sum_{j,i \neq j} I_{j\beta}) \}} \quad (I2)$$

Eliminating the 4 from both the numerator and the denominator in the right-hand side of (I2), we recover the quad clustering coefficient  $C_i^q$  as defined in Eq. (13), which completes the derivation.

- <sup>1</sup>M. E. Newman, A.-L. E. Barabási, and D. J. Watts, The structure and dynamics of networks. (Princeton university press, 2006).
- <sup>2</sup>A.-L. Barabási and M. Pósfai, Network Science (Cambridge University Press, 2016).
- <sup>3</sup>S. N. Dorogovtsev and J. F. Mendes, The nature of complex networks (Oxford University Press, 2022).
- <sup>4</sup>F. Battiston, G. Cencetti, I. Iacopini, V. Latora, M. Lucas, A. Patania, J.-G. Young, and G. Petri, “Networks beyond pairwise interactions: structure and dynamics,” *Physics Reports* **874**, 1–92 (2020).
- <sup>5</sup>D. J. Watts and S. H. Strogatz, “Collective dynamics of ‘small-world’ networks,” *nature* **393**, 440–442 (1998).
- <sup>6</sup>R. Albert and A.-L. Barabási, “Statistical mechanics of complex networks,” *Reviews of modern physics* **74**, 47 (2002).
- <sup>7</sup>E. Ravasz and A.-L. Barabási, “Hierarchical organization in complex networks,” *Physical review E* **67**, 026112 (2003).
- <sup>8</sup>A. Barrat and M. Weigt, “On the properties of small-world network models,” *The European Physical Journal B-Condensed Matter and Complex Systems* **13**, 547–560 (2000).
- <sup>9</sup>T. Opsahl, “Triadic closure in two-mode networks: Redefining the global and local clustering coefficients,” *Social networks* **35**, 159–167 (2013).
- <sup>10</sup>J. C. Brunson, “Triadic analysis of affiliation networks,” *Network Science* **3**, 480–508 (2015).
- <sup>11</sup>A. P. Kartun-Giles and G. Bianconi, “Beyond the clustering coefficient: A topological analysis of node neighbourhoods in complex networks,” *Chaos, Solitons & Fractals: X* **1**, 100004 (2019).
- <sup>12</sup>D. H. Serrano and D. S. Gómez, “Centrality measures in simplicial complexes: Applications of topological data analysis to network science,” *Ap-*

- plied Mathematics and Computation* **382**, 125331 (2020).
- <sup>13</sup>H. Yin, A. R. Benson, and J. Leskovec, “Higher-order clustering in networks,” *Physical Review E* **97**, 052306 (2018).
- <sup>14</sup>P. G. Lind, M. C. González, and H. J. Herrmann, “Cycles and clustering in bipartite networks,” *Physical review E* **72**, 056127 (2005).
- <sup>15</sup>P. Zhang, J. Wang, X. Li, M. Li, Z. Di, and Y. Fan, “Clustering coefficient and community structure of bipartite networks,” *Physica A: Statistical Mechanics and its Applications* **387**, 6869–6875 (2008).
- <sup>16</sup>M. Kitsak and D. Krioukov, “Hidden variables in bipartite networks,” *Physical Review E* **84**, 026114 (2011).
- <sup>17</sup>W. Jeong and U. Yu, “Effects of quadrilateral clustering on complex contagion,” *Chaos, Solitons & Fractals* **165**, 112784 (2022).
- <sup>18</sup>M. Jia, B. Gabrys, and K. Musial, “Measuring quadrangle formation in complex networks,” *IEEE Transactions on Network Science and Engineering* **9**, 538–551 (2021).
- <sup>19</sup>S. G. Aksoy, T. G. Kolda, and A. Pinar, “Measuring and modeling bipartite graphs with community structure,” *Journal of Complex Networks* **5**, 581–603 (2017).
- <sup>20</sup>F. Malizia, S. Lamata-Otín, M. Frasca, V. Latora, and J. Gómez-Gardeñes, “Hyperedge overlap drives explosive collective behaviors in systems with higher-order interactions,” *arXiv preprint arXiv:2307.03519* (2023).
- <sup>21</sup>G. Lee, M. Choe, and K. Shin, “How do hyperedges overlap in real-world hypergraphs?-patterns, measures, and generators,” in *Proceedings of the web conference 2021* (2021) pp. 3396–3407.
- <sup>22</sup>P. Jaccard, “Étude comparative de la distribution florale dans une portion des alpes et des jura,” *Bull Soc Vaudoise Sci Nat* **37**, 547–579 (1901).
- <sup>23</sup>G. Bianconi and M. Marsili, “Loops of any size and hamilton cycles in random scale-free networks,” *Journal of Statistical Mechanics: Theory and*

Experiment **2005**, P06005 (2005).

<sup>24</sup>M. E. J. Newman, S. H. Strogatz, and D. J. Watts, "Random graphs with arbitrary degree distributions and their applications," *Phys. Rev. E* **64**, 026118 (2001).

<sup>25</sup>T. Coolen, A. Annibale, and E. Roberts, *Generating random networks and graphs* (Oxford university press, 2017).

<sup>26</sup>G. Fagiolo, "Clustering in complex directed networks," *Physical Review E* **76**, 026107 (2007).

<sup>27</sup>M. E. Newman, "The structure and function of complex networks," *SIAM review* **45**, 167–256 (2003).

<sup>28</sup>A. R. Benson, R. Abebe, M. T. Schaub, A. Jadbabaie, and J. Kleinberg, "Simplicial closure and higher-order link prediction," *Proceedings of the National Academy of Sciences* **115**, E11221–E11230 (2018).

<sup>29</sup>J. Kunegis, "Konect: the koblenz network collection," in *Proceedings of the 22nd international conference on world wide web*

(2013) pp. 1343–1350.

<sup>30</sup>A. E. Mislove, *Online social networks: measurement, analysis, and applications to distributed systems* (Rice University, 2009).

<sup>31</sup>W. Kan, "What's cooking?" (2015).

<sup>32</sup>Scott Chacon, "The 2009 github contest," <https://github.com/blog/466-the-2009-github-contest> (2009), [Online; accessed June-2023].

<sup>33</sup>I. Amburg, N. Veldt, and A. Benson, "Clustering in graphs and hypergraphs with categorical edge labels," in *Proceedings of The Web Conference 2020* (2020) pp. 706–717.

<sup>34</sup>G. Ward, "Moby thesaurus ii," Project Gutenberg Literary Archive Foundation (2002).

<sup>35</sup>P. D. Karp, R. Billington, R. Caspi, C. A. Fulcher, M. Latendresse, A. Kothari, I. M. Keseler, M. Krummenacker, P. E. Midford, and Q. Ong, "The biocyc collection of microbial genomes and metabolic pathways," *Briefings in bioinformatics* **20**, 1085–1093 (2019).